T.C.

TED UNIVERSITY

GRADUATE SCHOOL

MECHATRONICS ENGINEERING

COGNITIVE MODELLING AND ANALYSIS OF JOINT IMPROVISATION MODALITY USING THE EXPERIMENTAL DATA

ATACAN DUMAN

ANKARA, 2023

COGNITIVE MODELLING AND ANALYSIS OF JOINT IMPROVISATION MODALITY USING THE EXPERIMENTAL DATA

A Thesis Submitted To
The Graduate School
of
TED University

by

Atacan Duman

In Partial Fulfillment of The Requirements
For
Master of Science
in
Mechatronics Engineering

ANKARA, 2023

I hereby declare that all information in this document has been obtained and presented in accordance with academic rules and ethical conduct. I also declare that, as required by these rules and conduct, I have fully cited and referenced all material and results that are not original to this work.

Name, Last name: Atacan Duman

Signature :

ABSTRACT

COGNITIVE MODELLING AND ANALYSIS OF JOINT IMPROVISATION MODALITY USING THE EXPERIMENTAL DATA

Atacan Duman

Master of Science, Mechatronics Engineering

Supervisor: Kutluk Bilge Arıkan

January 2023

How does physical interaction affect predictive behavior in biological movements? In this thesis, the movements of human and mammalian neural network-inspired virtual players are observed with improviser and follower models using the mirror game paradigm joint improvisation modality. The main purpose of this thesis is to show the improvement of motion estimation in humans by using different haptic information scenarios. Using mathematical metrics, higher complexity of tactile interaction between improvisers has enhanced improvisation performance over two suggested set-ups.

Keywords: Mirror game paradigm; Interpersonal Coordination; Haptic Interaction; Virtual Player; Joint Improvisation; Joint Action

ÖZET

DENEYSEL VERILER KULLANILARAK ORTAK DOĞAÇLAMA MODALITESININ BILIŞSEL MODELLENMESI VE ANALIZI

Atacan Duman

Master of Science, Mekatronik Mühendisliği

Tez Yöneticisi: Kutluk Bilge Arıkan

Ocak 2023

Fiziksel etkileşim, biyolojik hareketlerdeki tahmini davranışı nasıl etkiler? Bu tezde, insan ve memeli sinir ağlarından ilham alan sanal oyuncuların hareketleri, ayna oyunu paradigması ortak doğaçlama yöntemi kullanılarak, doğaçlama ve takipçi modelleri ile gözlemlenmiştir. Bu tezin temel amacı, farklı dokunsal bilgi senaryoları kullanarak insanlarda hareket tahmininin gelişimini göstermektir. Matematiksel ölçümlerden faydalanarak, doğaçlama yapanlar arasındaki dokunsal etkileşimin karmaşıklığı ile, önerilen iki kurulum üzerinden senkronizasyon performansını artırdığı gözlemlenmiştir.

Anahtar Kelimeler: Ayna Oyunu Paradigması; Kişiler Arası Koordinasyon; Dokunsal Etkileşim; Sanal Oyuncu; Ortak Doğaçlama; Ortak Eylem

ACKNOWLEDGMENTS

I would like to express my heartfelt gratitude to my supervisor Kutluk Bilge Arıkan for his invaluable guidance throughout the course of this research project. He has been a constant source of motivation and has provided insightful suggestions and comments that have helped shape this thesis into its present form. I am deeply thankful to him for being a constant source of support and encouragement.

I am truly blessed to have such an amazing and loving family who have stood by me through thick and thin, and I will forever be grateful for all they have done for me. I am deeply thankful for their sacrifices and for always being there for me. This acknowledgement would not be complete without mentioning each and every one of their names, Arzu Duman, Bülent Duman and Özgür Sarıca Thank you from the bottom of my heart.

I would like to extend my heartfelt thanks to the sweetest and most loving person in my life, Özlem Gündoğmuş. Your unwavering support, encouragement, and love have been the strawberries on top of my shortcake, making this journey a delightful experience. Your belief in me and your constant motivation have been my source of strength and inspiration. This thesis would not have been possible without your love and support. Thank you for being my best friend, and my partner in life.

I express gratitude to my lab mates Önay Karaca, Umut Candan and Amr Okasha for their support in this project. Their teamwork, expertise, and commitment inspired me. Thank you for sharing your knowledge, being supportive, and for the positive impact on my life. Your friendship is appreciated.

I would like to extend my heartfelt thanks to the friendships I have won throughout my life that not leaving me alone and being a part of this work, Mert Gündüz, Serkan Erol, Önen Emre Can, Devrim Kara, Murat Alp Korkut, Onur Safran, Beste Akdere, Emre Kasar, Mert Işık, Emre Ekinci, Utku Akgüneş, Can Canan, Ahmethan Deniz, Gökmen Akan, Müge Uzun, Turhan Böler, Hüseyin Caner Oflaz and BODES Band.

To My Parents…

TABLE OF CONTENTS

LIST OF TABLES

TABLES

LIST OF ABBREVIATIONS

MG	Mirror Game
SI	Social Interaction
JI	Joint Improvisation
LF	Leader Follower
HI	Haptic Interaction
HI+	Haptic Interaction activated
HI-	Haptic Interaction not activated
VP	Virtual Player
HP	Human Player
IMS	Individual Motor Signature
HRI	Human-Robot Interactions
SAR	Socially Assistive Robot
ADS	Autism Spectrum Disorder
AlterEgo	AlterEgo European Project
CC	Co-Confident
HKB	Haken-Kelso-Bunz
PD	Proportional Derivative
HKB	Haken-Kelso-Bunz
CV	Circular Variance
RMS	Position Temporal Correspondence
EMD	Earth Mover's Distance

E	Entropy
PDF	Probability Density Function
CDF	Cumulative Distribution Function
THJI	Target Human Joint Improvisation
HDHJI	Human Driven Haptic Joint Improvisation
TDHJI	Target Driven Haptic Joint Improvisation
TJI	Triad Joint Improvisation
tDCS	Transcranial Direct Current Stimulation

LIST OF FIGURESS

FIGURES

CHAPTER 1

INTRODUCTION

Social interaction (SI) is a reciprocating and coordinated act of imitating, decoding, and influencing the actions of others [1]. It is a foundation block of human society that is highly influenced and linked to verbal communication and bodily motions. Those naturally developed mechanisms help humanity to correctly infer shared goals, beliefs, and feelings of others; with the correctly defined intentions, we fall in synchrony to create organizations, structures and accomplish mutual goals.

However, people that are not typically developed have drawbacks connecting with those who are typically developed; also, most disorders are exacerbated or caused by a lack of social interaction. Because of attenuated levels of interaction, people with special needs are excluded from society. Those impairments can be cured by training in social skills or bodily motions that often occur during social interactions. Persons with special needs exhibited different movement characteristics in social interaction-based game paradigms compared to typically developed persons [2-6]. Virtual playmates that can interact regardless of psychological status and bodily motion rehabilitation during social interaction may be beneficial for people who are in need of bridging the gap between interaction with peers.

1.1 Motivation

The mirror game paradigm can be considered an intuitive and easygoing social interaction monitoring method. Paradigm mainly consists of two distinct game modes, namely Leader-Follower, where one of two participants is designated with a leadership role, and Joint Improvisation, where there is no designated leader, and two participants improvise freely.

This thesis motivated replacing one of two players with a human central nervous system-inspired virtual playmate, that can mimic its partners' movement characteristics, or a typically developed persons, for playing regardless of psychological status, and implementing haptic interaction to mirror game for bodily movement rehabilitation. This kind of build-up may cover the topics of early diagnosis of physiological disorders and repairing social interaction dynamics by using haptic interaction.

1.2 Research Background

Social interactions are an inevitable part of human lives; that phenomenon often occurs in joint actions such as hunting, cooking, and playing games with coordinated participation patterns; for generating a well-played and coordinated series of movements, humans tend to create representations of his/her partners' upcoming movements, more you spend time with them better you coordinate or predict what the next step is going to be [7].

When two individuals interact physically in joint actions, people create haptic information channels [8-9]. To use an example, consider a parent assisting an infant as they learn to walk. Due to the haptic information flow between parent and kid during a physical engagement, children who interact with their parents physically tend to have better motor control. [10].

Mirror game provides a simple and effective representation of joint human action for studying social interaction impairments of people that are not typically developed. Literature of mirror game built on gathering data on typically developed and non-typically developed persons with two distinct modalities as Leader-Follower and Joint improvisation, introduced in [11].

People with developmental challenges may showcase a unique and extraordinary way of movements. For instance, those who have faced childhood trauma exhibited a more cautious and methodical approach to movements, those with anxiety brought a different perspective to leading interactions, and many other disorders showed different movement patterns varying on the diagnosis [2-6].

Also, another work area is coming up with human-like virtual playmates that can exhibit human movement patterns. Locking in synchrony via using non-linear coupled oscillators is well studied. One of the highlights is using a well-validated mathematical model named Haken, Kelso, and Bunz Model (HKB). Combining Vander-Pol and a

Rayleigh oscillator [12], another highlight is the PCFE algorithm offered in [11], also a mammalian rhythmic movement pattern generation system inspired model; programmable central pattern generator (CPG) that employs coupled non-linear Hopf oscillators in [13] stand out for human-like playmates.

Even though the proposed models exhibited human-like lock-in synchrony, they lacked a phenomenon called “exit from synchrony” during social interactions. Later, this under-studied phenomenon was studied in [14] by coming up with a novel mathematical model that was implemented in HKB and PCFE models.

However, exit from synchrony hasn’t displayed turn-taking, improvising aspects of joint improvisation modality. The existence of individual motor signatures shown in [15] has unlocked the human-like improvisation and leading kinematics of mirror game virtual agents; also, in [16], it has been demonstrated that people with closer individual motor signatures showed better synchronization and game performance in mirror games. Later, individual motor signature has implemented as velocity time series to a novel joint improvisation algorithm with an HKB oscillator [17].

1.3 Scope of Thesis

This study provides and overview of how haptic interaction (HI) between human and virtual players improves tracking performance in the Joint Improvisation modality of Mirror Game. Several metrics are used to study different haptic interaction scenarios and how game performance and prediction enhance for bodily movement rehabilitation. Accordingly virtual improviser player is developed using programmable central pattern generator with the exit from synchrony and individual motor signature (IMS) terms to mimic highly varying dynamics of joint improvisation modality in the mirror game. Two different experimental set-ups with eight different interaction scenarios in total are developed to study haptic interaction in a mirror game.

CHAPTER 2

LITERATURE SURVEY

Social interaction is a foundation block of human lives with solid evolutionary roots. It can be defined as a real-life, complex phenomenon. Social cognitive neuroscience has been investigating basic social abilities for regular human lives, such as recognizing, attention, recalling socio-emotionally pertinent stimuli, and the effects of human perception on social interaction. For example, a person's face contains socially relevant cues, such as emotional expressions, that can be used to make implicit or explicit judgments by humans [18-20]. Trustworthiness [21], racial identification [22], and effects of facial appeal [23].

In addition, a stream of studies has shown bodily motions obligatory for naturally developed social interaction. That necessity stands for the importance of decoding social signals in the form of biological motion (body movements). It has been an essential pathway to understanding the phenomenon. Another mechanism unveils as the Synchronization of Bodily motions, verbal expressions, or both spontaneously emerge in time to build a healthy interaction when people lock in social interaction [24].

Another vital research on social interaction shows the existence of 'mirror neurons' in monkeys [25-26]. Mirror neurons are excited when a monkey is being displayed to someone else's specific action, as well as when the monkey performs that action displayed previously. Due to its apparent importance for social interactions, the discovery of mirror neurons generated much attention. Furthermore, mirror neurons unlocked the thoughts of being a critical component of representing the goals of intentions of others; this work also displays the importance of linking Bodily movements to social interaction in a cognitive manner.

The study of social interaction is concerned with how two brains reciprocally affect one another through encounters, which requires a bi-directional approach—for example, building a joint action through shared goals or intentions in synchronous, fine-grained ways to please each other. Some joint actions require expertise in that specific area to lock in successfully [27], a chorus singing, surgical team saving the life of another, funny enough even though we perform joint tasks daily, e.g., holding the door and noticing someone behind you, passing a tea to a friend, we hardly notice them. Any social synchrony failure urges an instant frustration; we quickly notice something is wrong and can't name the feeling of impairment, such as carrying weight to gather and one having trouble following the rhythm [28].

Prior research has shown that during joint actions, co-actors not only plan for individual movements but create representations of the partner as performing his/her movements [29]. Forming representations of each other is a vital tool of the mind that can remove interferences between movements [30] and facilitate coordination performance [31] and imitation [32]. It also has its dynamics, such as prioritizing partners' movements before his/her own [33].

To synchronize, forming representations is not the only tool for a thriving SI. Prediction is another crucial component that decreases participants' effort to represent partners in mind and focus more on individual performance [34]. Increased prediction capability grants the individual increased self-esteem and more creativity; for example, in salsa dance, the male participant performs more straightforward movements making the male dancer more predictable, which helps the female dancer to improvise, and dance more freely and confidently [35]. Also, it is a reversible process for better performance, e.g., the more unpredictable you are better you perform in a football match [36].

However, people do not always have the necessary information to build instant and mutual goals, at that times we have to create real-time solutions for situations and improvise to achieve the desired output, e.g., you forgot an essential ingredient for dinner, and you can't make it on time if you go back to the grocery, or there is a traffic jam along the way, and you take another route to work [37], improvisation is an often bi-directional, joint action as well, e.g., you saw an old friend and engaged in a small talk, you jointly improvise, try to create representations of each other, and a good synchronization can end up arranging a date some time and catch-up to strengthening the social bonds again. In joint improvisation, co-actors undergo multi-modal, reciprocal, and open-ended interactions in real-time without having a "designated leader" [11] and planning their own movements [38].

In addition to Human-Human SI, human-robot social interaction (HRI) is an important phenomenon to study with rehabilitative manners to assist those in need, both physical and social/emotional. Physically interacting robotics have been studied in manipulation and haptic areas. On the other hand, Social/emotional robotics contains three main research areas: assistive robotics, social robotics, and socially assistive robotics (SARs). All areas of studies have oral and non-verbal interaction with partners [39]. Positive outcomes have been held by many application areas, such as teaching autism spectrum disorder children daily tasks such as eating and hugging someone, bridging the gaps of social impairment by repetitive synchronous movements [40], or assisting post-stroke patients in re-using limb functions through repetitive synchronous movements [41]. With demonstrated gap-bridging ability of SARs developing human-like moving robots became important for better interaction to keep the rehabilitative manner of SARs at peak level with a controlled environment that researchers can experiment with and look for new interaction scenarios to repair and understand.

Repairing bodily motions persistently would be a key to awakening the feelings of healthy social interaction for those who have trouble adapting to society because of various non-typically developed human being-related situations, e.g., autism spectrum disorder, schizophrenia, and anxiety. In literature, people that are not typically developed showed different movement patterns, such as people with childhood trauma showed lower levels of risk-taking and entropy/complexity with their movements [2], people suffering from anxiety showed attenuated levels with leading the interaction [3], people have schizophrenia had motor coordination problem [4], and [5] suggested that detecting interpersonal coordination impairments might be a good way for early diagnosis with schizophrenia also persons with ADHD showed distinctive patterns of synchronization [6].

Regarding the highly varying movement pattern impairments of not typically developed persons, developing an intuitive and easygoing monitoring rehabilitation protocol became a challenge for researchers. The European Project "AlterEgo" [42] has been a great spark to bring researchers' attention onboard. This thesis has been offered to cover both "easygoing" and "intuitive" natural bodily movement rehabilitation set-up.

The mirror game paradigm provides an "easygoing" and "intuitive" to study/monitor social interactions with motor coordination skills are the primary goal of the proposed data collection method, with a strategy that is" dependent on two players move handles along parallel tracks and are asked to create synchronized bodily motions—mainly containing two different modalities as Leader-Follower (LF) and Joint Improvisation (JI). Nature of LF mode designed with designated leaders on the game, i.e., one co-actor given the role of leading the motion and the other as following with minimum temporal delays. The nature of JI emerges when there is no designated leader. Coactors generates curiously generated movements that the leadership during game rounds unintentionally change, regarding the comments of co-actors like "I did not understand who is leading" [11,42]. Other than leading and following sub-level interaction, a rare state of life [42] could be monitored as a co-confident motion. These moments of "togetherness" or generation of "we-space" basically can be explained as co-actors' adaption to their temporal delays resulting in pure synchronized states where the leader disappears. They move as one, and the heart rate increase as markers of psychology [37], feeling the joy of synchronizing [42-43]. Even though the suggested paradigm shows substantial aspects of social humanity, it lacks bodily movement rehabilitation.

In the scope of this thesis, an emerging topic, Haptic Interaction, has been offered for joining the body moving rehabilitation. It is a strong phenomenon that takes its place from the infant stages of human lives, where a parent teaches the infant how to walk by parent letting the infant hold their parents' hand or arm to advance motor control [45]; that kind of information change between parent and infant remains unknown [45-46]. Prior research has shown that haptic interaction enabled tracking tasks via virtual springs and dampers enhanced human prediction and performance of tracking tasks [47]. Therefore, adding haptic feedback to human movements has been a good candidate for repairing human coordination in different means. For instance, Brezis and colleagues investigated patterns of joint improvisation for typically developed (TD) and autistic people, and they reported that autistic participants showed attenuated levels of co-confident motion, i.e., synchronization stability has lowered [48]. That can be linked to prior research that suggests haptic forces helped co-actors to stay in synchrony, i.e., increased synchronization stability [49-50]. Therefore, such a situation leaves the question, “Can we rehabilitate autistic children by improving synchronization stability via haptic coupled mirror game?” or “How do haptic interaction parameters affect the social dynamics of mirror game to repair different movement characteristics of non-typically developed humans?”.

The proposed data collection method (Mirror Game), inspired by theater practice [11], had an open challenge for developing human-like moving virtual agents, which is a popular topic for many application areas of human-robot interaction. Regarding the highly non-linear characteristics of bodily movements, different applications of coupled non-linear oscillators have been proposed [51-54]. One critical model for Human movement characteristics is a well-validated mathematical model named Haken, Kelso, and Bunz Model (HKB). Combining Vander-Pol and a Rayleigh oscillator [12]. It aimed to model asymmetric and symmetric human hand movements with coupling parameters with the well-validated nature of HKB. The model has been intensively used to model virtual agents both for leader-follower and joint improvisation modalities.

The first objective of the related work is to define the intrinsic dynamics of the virtual player by using the HKB equation:

Defining a double integrator:

$$\ddot{x} = u \tag{1}$$

Damped harmonic oscillator:

$$\ddot{x} = a\dot{x} + bx = u \tag{2}$$

HKB oscillator [12]:

$$\ddot{x} + (ax^2 + \beta\dot{x}^2 - \gamma)\dot{x} + \omega^2 x = u \tag{3}$$

Combined final model:

$$\ddot{x} + \left(\alpha x^2 + \beta \dot{x}^2 - \gamma\right)\dot{x} + \omega^2 x = [a + b\left(x - r_p\right)^2]\ (\dot{x} - r_v) \qquad (4)$$

Virtual agents' position, velocity, and acceleration are given as x, $\dot{x}$, $\ddot{x}$ Respectively. r_p denotes recorded human position and r_v As human player velocity. α, β, γ, and ω deployed as oscillator parameters. a and b act as non-linear coupling parameters that equal the velocity between co-actors.

Optimal control strategy with minimizing cost function with HKB has been the most successful among others, such as adaptive and traditional PD control [55].

However, developed structures had only the ability to follow, not lead or improvise, to arm virtual agents with those capabilities existence of Individual Motor Signature (IMS) has been a great tool to add human behaviors to virtual agents that can improvise and lead. IMS defined the human movement characteristics in mirror game that every person has their unique motor signature [15]. To define the unique motor signature of people, a new game mode has been added to the mirror game named "solo round" this game mode asks players to create motions how they like on the mirror game set-up without a partner. Then they calculated the probability distributions of solo round velocities, i.e., the probability of playing the game with specific velocities [15].

Later, researchers claimed that people with closer IMS showed better results in means of synchronization and game performance [16]. Distance between individual motor signatures has been calculated using a new metric named Earth Movers Distance (EMD).

Regarding the work carried out by [15] and [16], a new novel joint improvisation virtual partner has been offered using the velocity time series of solo rounds. Applying the velocity time series that is used to calculate dyads' motor signatures to virtual agents resulted granted the capability of leading and improvising [17].

Alternative to the HKB oscillator, a predictor-corrector model is offered [11] for joint improvisation with a new "exit from synchrony" term [14]. It has been said that the current virtual agent architectures' in-phase and anti-phase movements are well studied; however current designs lock-in synchrony staying there forever and commented it is "quite boring while playing." During Human player-human player mirror game interactions and social life itself, people go in and out of synchrony all the time; emphasizing the in-and-out nature of synchrony, researchers came up with a new mathematical definition named “exit from synchrony.” [14]:

$$\frac{df_i}{dt} = -nf_i + \beta_i \frac{v_j}{1 + \frac{E}{E_0}} \xi_i \tag{5}$$

To define the error E in the proposed exit term, the RMS error of the velocities v_1 and v_2, integrated over time τ. Squared differences of velocities D and squared sum of velocities S are calculated to define E.

$$\frac{dD}{dt} = (v_1 - v_2)^2 - \frac{D}{\tau} \tag{6}$$

$$\frac{dS}{dt} = (v_1 + v_2)^2 - \frac{S}{\tau} \tag{7}$$

Their ratio:

$$E = \frac{D}{S + \epsilon} \tag{8}$$

Where $v_1$is the counterparts’ velocity, v_j and v_2 VP velocity, ξi is the noise term and β_i, n, E_0 controllable tuning parameters. The model basically increases noise gain if the velocity difference is small, acting as a drift over the opposing players’ reference position. The exit-from synchrony term has been implemented in HKB and the predictor-corrector model (PCFE Model):

In the predictor-corrector model change rate of player velocity v_1 has given by a corrector term $z_1(t)$ and a predictor that is dependent on the sum of periodic function amplitudes $B_{1n}(t)$ varying over time.

$$\dot{x} = \sum_n B_{1n} \omega n cos(\omega nt) + z_1(t) \tag{9}$$

The tracker v_1 and stimulus v_2 velocity error is integrated by the corrector l_1 defines jitter pattern frequencies on track.

$$\dot{z_1} = l_1(v_2 - v_1) \tag{10}$$

The predictor amplitudes B_{1n} adapts the corresponding frequency components of the stimulus, B_{2n}, with rate k.

$$\dot{B_{1n}} = k\left(v_2 - \sum\nolimits_m B_{1m}\sin(wmt)\right)\sin(\omega nt) \quad (11)$$
$$n, m = 1, 2, 3 \ldots$$

Combined PCFE Model from [11] and exit from synchrony term (5) from [14]:

$$\dot{x} = \sum\nolimits_n B_{1n}\omega n cos(\omega nt) + z_1(t) + \boldsymbol{f}(\boldsymbol{t}) \quad (12)$$

And The HKB Model:

$$\ddot{x} + (\alpha x^2 + \beta\dot{x}^2 - \gamma)\dot{x} + \omega^2 x = [a + b\left(x - r_p\right)^2]\,(\dot{x} - r_v) + \boldsymbol{f}(\boldsymbol{t}) \quad (13)$$

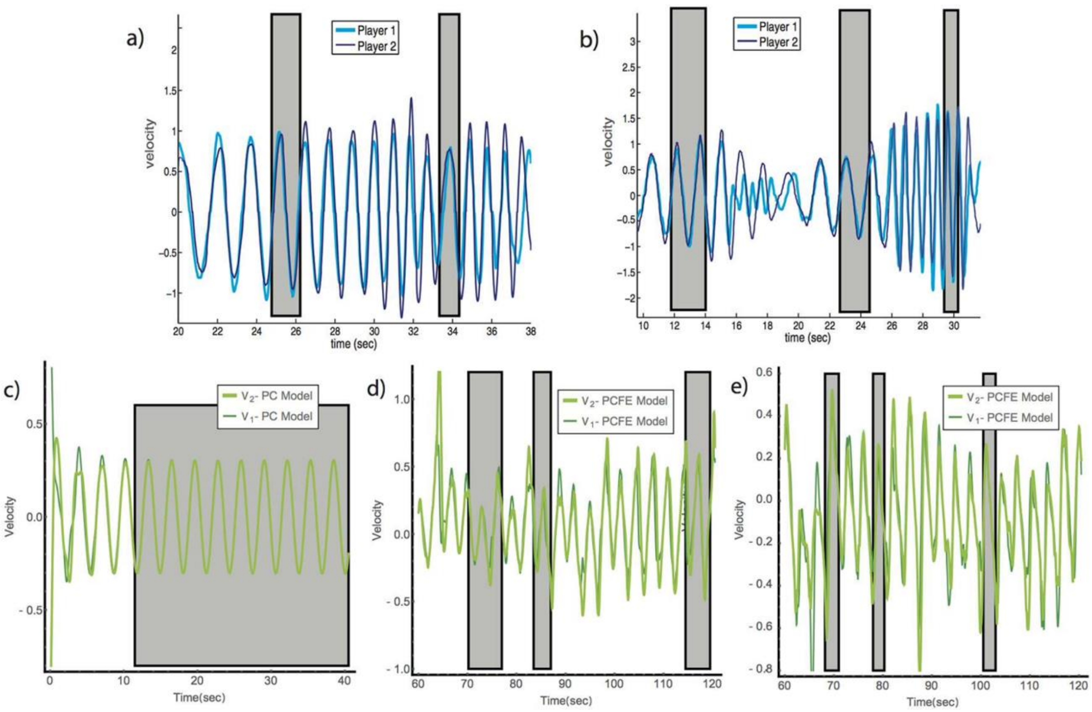

Fig 2.1 Mirrored PCFE models capture key aspects of human joint improvised motion in the mirror game [14]

Here Fig 2.1 shows outputs of PCFE Model outputs with the exit from synchrony term, (a) and (b) shows human dyadic interaction. Gray boxes show areas of co-confident motion showing that the VP-VP round shown on the graph (d) and (e) had similar properties with human player rounds with the means of co-confident motion. Models with PCFE showed 8.5±3% CC over the game rounds and correlated that output to findings on [56] saying that players go in CC motion averaged 9±2% over the game rounds ranging from 3% to 14%.

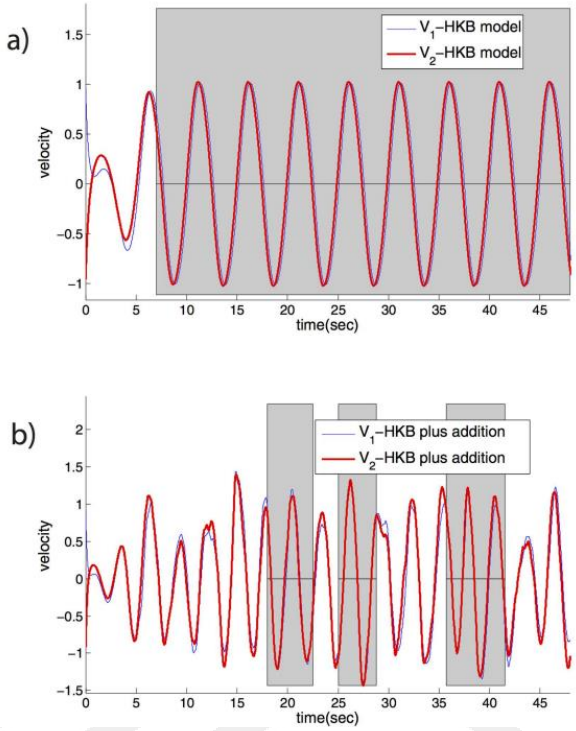

Fig 2.2 HKB with and without exit from synchrony term [14].

Fig 2.2 (a) shows infinite synchrony without exit from synchrony, and (b) shows the HKB model with exit term with close results shown in the literature regarding CC.

However, even though the model shows under and overshoots mimicking human-like behaviors, the applied experience of exit from the synchrony model showed a lack of leadership for joint improvisation modality.

In this thesis novel virtual player that is made of programmable central pattern generators (CPGs) developed in [13] combined with the introduced exit from synchrony term introduced in [14] and Individual motor signature in [17] to capture human-like turn-taking and synchronize.

Central pattern generators (CPGs) are biological neural circuits that can self-organize to create rhythmic outputs without receiving rhythmic input [57] and are employed with daily tasks of human lives such as walking, chewing, and breathing [58].

From the mammalian nervous system, the working principle of CPGs in [59] by experimental work done on cats are given as:

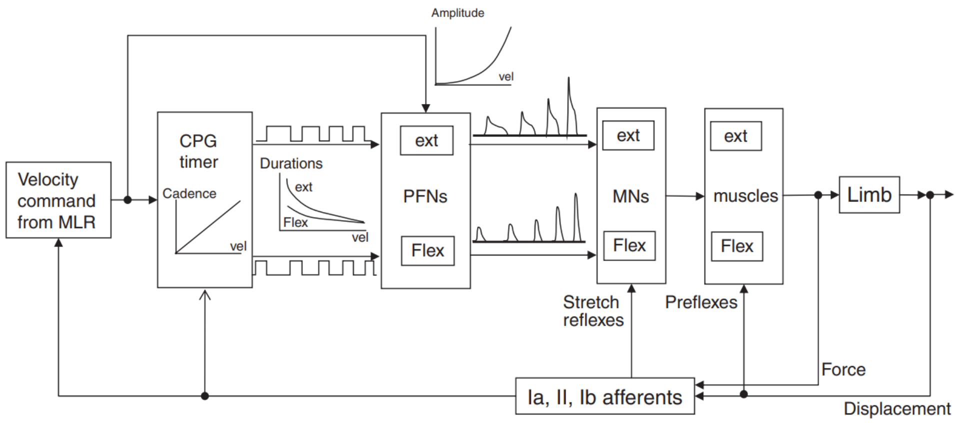

Fig 2.3 Mammalian rhythmic movement generation by Central Pattern Generators [59].

Fig 2.3 provides a simplified representation of proposed movement mechanisms. Velocity command generated on the midbrain locomotor region (MLR) by a closed loop system with the aid of type la, ll, and lb afferents (nerve fibers) for the sake of simplicity, those nerve fibers acting as sensory feedback to measured movement outputs to midbrain and CPG timer to keep generating movement patterns. CPG timer region produces necessary phase durations and timing for extensor and flexor muscles. The information is transferred to CPG pattern-forming networks (PFNs) to adjust movement amplitudes of extensor and flexor muscles. Later pattern forming networks modulates Motor neurons (MNs). Activation of muscles given by Δx and the force is modulated by the intrinsic properties of muscles, e.g., damping and stiffness later output the limb movements.

In this study, the CPG pattern forming networks inspired movement generation system developed in [13] is used to come up with a mirror game virtual agent. The study [13] introduces architecture with coupled adaptive non-linear Hopf oscillators to control a 23 DOF humanoid robot’s movements. The proposed system can learn arbitrary rhythmic signals with a supervised learning framework using automatically adjusted parameters such as coupling weights, intrinsic frequencies, and amplitudes. The system shows the same dynamics even though the teaching signal is removed, and parameters stay embedded as the limit cycle of a dynamic system.

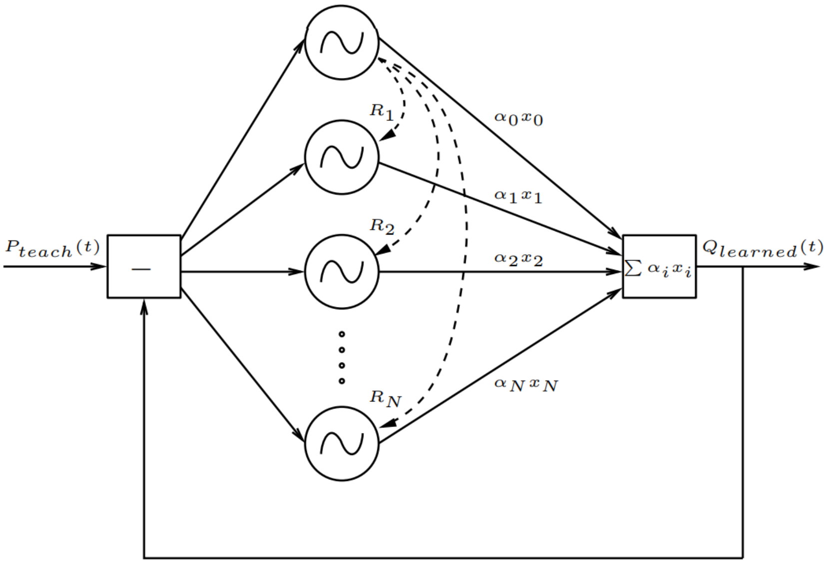

Fig 2.4 Hopf oscillator-based adaptive network proposed in [13]

Each oscillator fed with the same teach signal $F(t) = P_{teach}(t) - \sum_i \alpha_i x_i$ Which can be defined as an error to reference input. Term $\sum_i \alpha_i x_i$ is defined as $Qlearned(t)$. All oscillators receive scaled phase input R_i Except oscillator 0.

The equations describing CPG are as follows:

$$\dot{x}_i = \gamma(\mu - r_i^2)x_i - \omega_i y_i + \epsilon F(t) + \tau \sin(\theta_i - \phi_i) \tag{14}$$

$$\dot{y}_i = \gamma(\mu - r_i^2)y_i + \omega_i x_i \tag{15}$$

$$\dot{\omega}_i = -\epsilon F(t) \frac{y_i}{r_i} \tag{16}$$

$$\dot{\alpha}_i = \eta x_i F(t) \tag{17}$$

$$\dot{\phi}_i = \sin\left(\frac{\omega_i}{\omega_0}\theta_0 - \theta_i - \phi_i\right) \tag{18}$$

$$\theta_i = \operatorname{sgn}(x_i)\cos^{-1}\left(-\frac{y_i}{r_i}\right) \tag{19}$$

$$F(t) = P_{\text{teach}}(t) - Q_{\text{learned}}(t) \tag{20}$$

$$Q_{\text{learned}}(t) = \sum_{i=0}^{N} \alpha_i x_i \tag{21}$$

$$r = \sqrt{x^2 + y^2} \tag{22}$$

The parameters of the CPG system are represented by τ and ϵ, which are the coupling constants, and η, which is the learning rate. The output of the CPG, known as Q_{learned}, is determined by combining the output of each individual oscillator using a weighted sum. F(t) serves as a negative feedback mechanism, and the difference between Q_{learned} and P_{teach} tells us what the CPG still needs to learn. The amplitude of the frequency term ω_i is represented by α_i. The equation of evolution maximizes the correlation between x_i and F(t), this process continues until the frequency component ω_i is eliminated from F(t) due to the negative feedback loop. $\dot{\phi}_i$ denotes the phase difference between oscillator i and 0, which ultimately converges to the phase difference between the instantaneous phase of oscillator 0 and the instantaneous phase of oscillator i, represented by θ_0 and θ_{i}, respectively. To ensure proper phase relations, each additional oscillator is coupled to oscillator 0 with a strength term of τ. After convergence, F(t) equals zero, and all periodic signals remain the same, mimicking repetitive tasks.

To discuss the outputs of human-human and human-virtual partner interactions series of metrics have been proposed by researchers:

2.1 Metrics Developed for Mirror Game

2.1.1. Motion Complexity

Wavelet transform calculates LF and JI round motion complexity in MG set-ups [16].

$$\mathrm{X(a,b)} = \frac{1}{\sqrt{\mathrm{a}}}\int_{-\infty}^{\infty} \psi\left(\frac{\mathrm{t-b}}{\mathrm{a}}\right)\mathrm{x(t)dt} \tag{23}$$

where a is scaling, and b is time shift factor, x(t) represents input signal, and orthonormal wavelet is denoted as ψ.

2.1.2 Relative Phase

The relative phase between the players is calculated to verify the leader role in MG. Hilbert Transform is used to find the player's phase angle:

$$\phi(t_i) = \arctan\left(\frac{H_{1,2}(t_i)}{x_{1,2}(t_i)}\right) \tag{24}$$

where x_1 and x_2 denote the players' positions, t_i represents simulation time. The relative phase between players is found by:

$$RP = \phi_1(t_i) - \phi_2(t_i) = \arctan\left(\frac{H_1(t_i)x_2(t_i) - H_2(t_i)x_1(t_i)}{x_1(t_i)x_2(t_i) + H_1(t_i)H_2(t_i)}\right) \tag{25}$$

where $H_1(t)$ and $H_2(t)$ show the Hilbert transform of participants, respectively [60].

2.1.3. Detecting CC Periods

When the difference in velocity between the two stages, normalized by [11], exceeds 0.95 or the time gap between the peak occurrences surpasses 0.3 seconds [43], these periods are removed from the data, and what remains is considered to be CC motion.

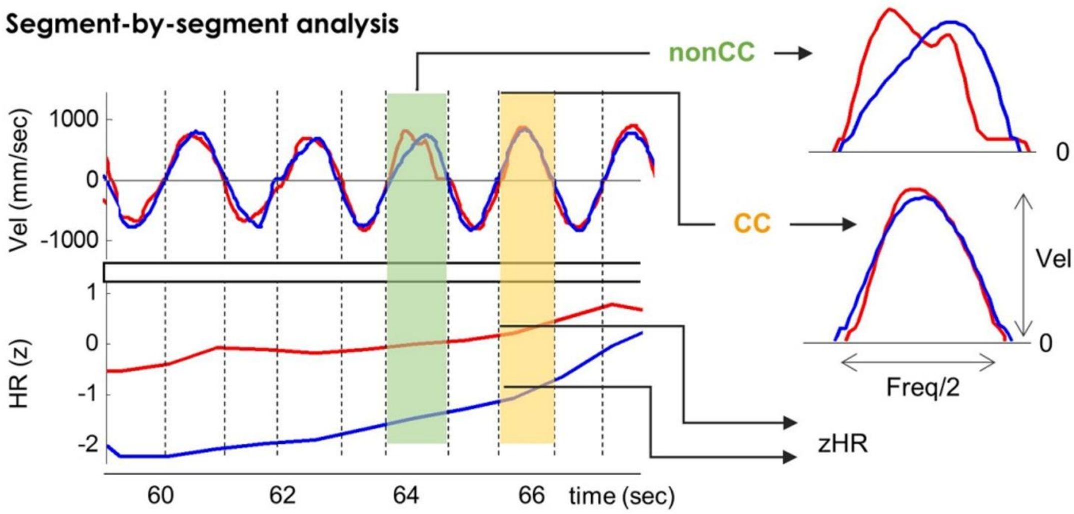

Fig 2.1.3.1 CC Versus nonCC Motion

Fig 2.1.3.1 shows co-confident motion versus non-co-confident motion segment-by-segment with change of velocity through the game round in [43].

2.1.4. Circular Variance (CV)

The amount of synchronization between the leader and followers is counted using the circular variance (CV) [55]:

$$CV = \left\| \frac{1}{k} \sum_{j=1}^{k} \exp\left(i\Delta\phi_j\right) \right\| \quad \in [0,1] \tag{26}$$

CV values are used to indicate the degree of synchronization between the players, where $\Delta\phi_j$ represents the relative phase between the players, and k denotes the number of time steps. A higher CV value indicates a greater level of synchronization between the players.

2.1.5. Position Temporal Correspondence (RMS)

The normalized position error between the leader and follower is defined by the root mean square (RMS) [17]. It refers to how well they coordinated their movements throughout the game.

$$RMS = \frac{1}{M} \sqrt{\frac{1}{n} \sum_{k=1}^{n} (x_{1,k} - x_{2,k})^2} \tag{27}$$

where M stands for the set of permitted locations, n for sample steps number throughout the simulation, and $x_{1,k}$ and $x_{2,k}$ refer for participants' positions.

2.1.6. The Earth Mover's Distance (EMD)

EMD used as calculating amount of adaptation throughout the game rounds, three levels of distance is calculated as $\eta(\sigma_i, \mu_i)$, $\eta(\sigma_j, \mu_j)$ and $\eta(\mu_i, \mu_j)$ where $\sigma_{i,j}$ players' solo round velocity PDF (IMS) and $\mu_{i,j}$ players' game round velocity PDF. To evaluate the adaptation between players, the Earth Mover's Distance is calculated as follows [17]:

$$EMD(PDF_1(z), PDF_2(z)) = \int_Z |CDF_1(z) - CDF_2(z)| dz \tag{28}$$

2.2 Contribution of Thesis

Here, this thesis offers a novel human like haptic follower and improviser robot arm deployed joint improvisation mirror game modality set-up with a novel human like virtual coactor to challenge human social interaction patterns.

- Novel virtual player for joint improvisation modality in mirror game.
- Implementation of haptic interaction with joint improvisation to mirror game.
- Adding a new modality that has three improvisers VP-VP-HP.
- A novel CC detection algorithm that can define leaders and followers during game rounds.
- Denoting effects of haptic interaction entropy/complexity to game performance.

CHAPTER 3

MATERIALS AND METHODS

Chapter 3 presents the quantitative approach used to examine the players' movement characteristics in the mirror game. This study offers two types of data collection methods: virtual (VE) and physical environment (PE) experimental rig. VE consists of two parallel tracks with ball avatars created in Simulink Virtual Environment (VR Sink). Each ball is controlled with an analog input u from a joystick. A virtual spring is implemented between ball avatars for haptic interaction. Also, vibratory feedback is added if players move too much away from each other, mimicking increased haptic force. On PE, the experimental rig consists of two physical parallel tracks made of rails deployed, with a target on the opposing side. On the human side, there is an extra 2DOF robot arm coupled with a modular soft spring to the human control handle. That kind of formation enabled us to experiment with different haptic interaction scenarios, including improvising as a triad.

3.1 Virtual Environment Experimental Rig

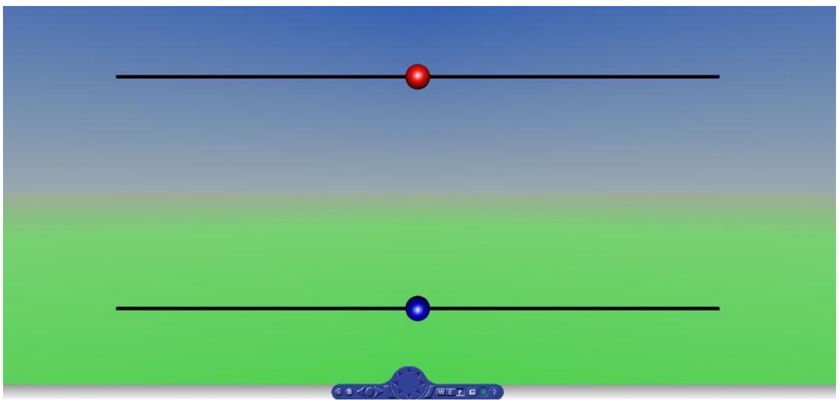

Fig 3.1.1. Virtual Environment

The input of the human players, u, is taken via the left joystick and used to drive the follower avatar end effector model through the following dynamics in Equation 29.

$$m\ddot{x}_{hp} + c\dot{x}_{hp} = u \tag{29}$$

where $\dot{x}_{hp}$ and $\ddot{x}_{hp}$ represent the human player's velocity and acceleration, respectively. The m and c system parameters form game dynamics. They are tuned regarding the easily adaptable nature of the mirror game. (m = 1 kg and c = 1.25 Ns/m).

Since the avatars are force controlled by using a joystick, damping c has been added to make it easier for the player to turn and move. The joystick's vibration motors, which produce a vibration whose amplitude is proportionate to the amplitude of the input owing to virtual elastic forces, provide the physical haptic feedback. The following equation models the virtual spring's relationship with spring stiffness, k:

$$F_h = k(x_2 - x_1) \tag{30}$$

where x_1 and x_2 denote player positions.

3.2 Physical Environment Experimental Rig

Physical Environment Experimental Rig provides a human-virtual player interaction modality with haptic interaction.

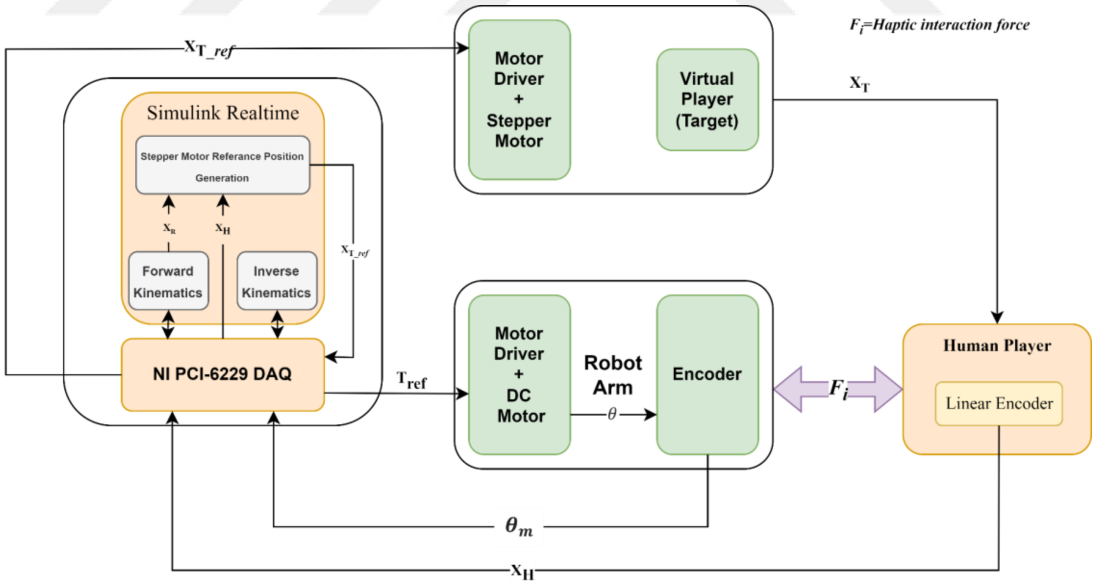

Fig 3.2.1 PE Experimental Rig Block Diagram

The target movement is produced by a stepper motor using a timing belt for linear actuation. The timing belt is equipped with a tightener mechanism, similar to a 3D printer, which allows for precise adjustments to the target movements, creating a closed-loop system that takes into account the step angles per rotation. The player side of the system features two carts, one for the human player and the other for the robot arm. These carts are connected via 8mm shafts to enable haptic interaction between them.

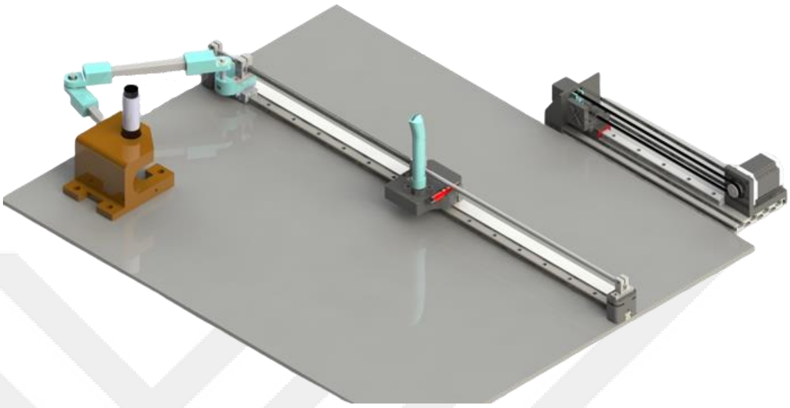

Fig 3.2.2 PE Experimental Rig

Haptic interaction is achieved by connecting robot and human handle carts with a specially designed spring. Haptic force computed over time depending on Δx between robot and human with a known stiffness(k).

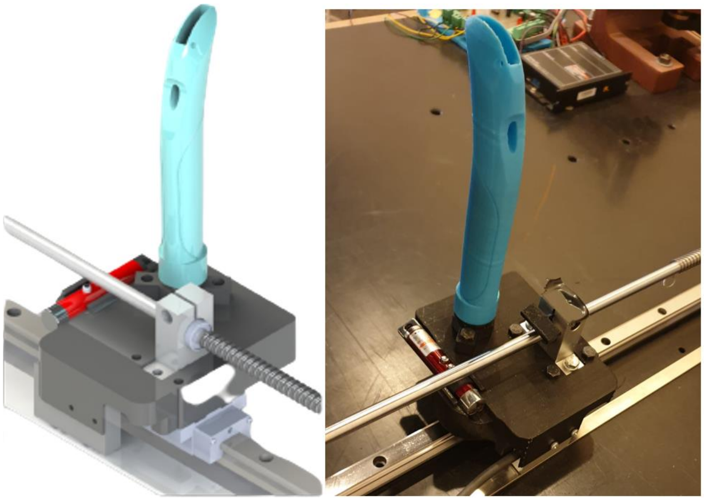

Fig 3.2.3 Human Handle

The player handle is designed with a rotating, ergonomic stick for improved grip and ease of use. A red laser has also been added to the handle cart to enable the human player to see their position relative to the target. The human player's movements are tracked by a linear encoder that is mounted on the handle cart.

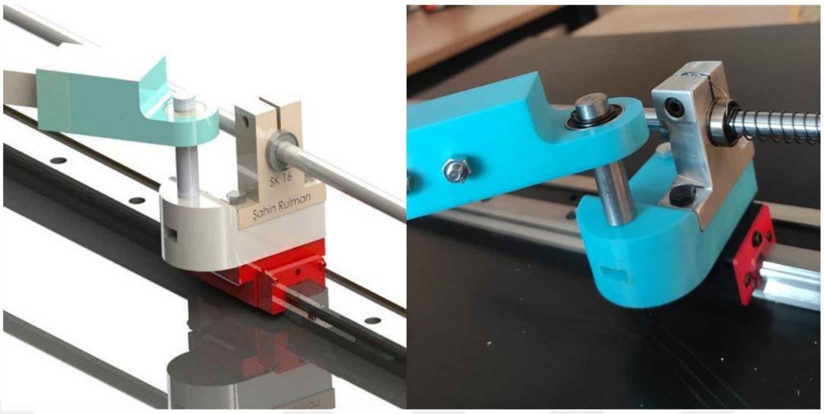

Fig 3.2.4 Robot arm cart

1 DOF robot arm drives the cart by a PID controller. The controller positions the cart on rail by using a kinematics model using the feedback of an encoder mounted on the EC-MAX motor.

Robot arm forward and inverse kinematics modelled as follow [61]:

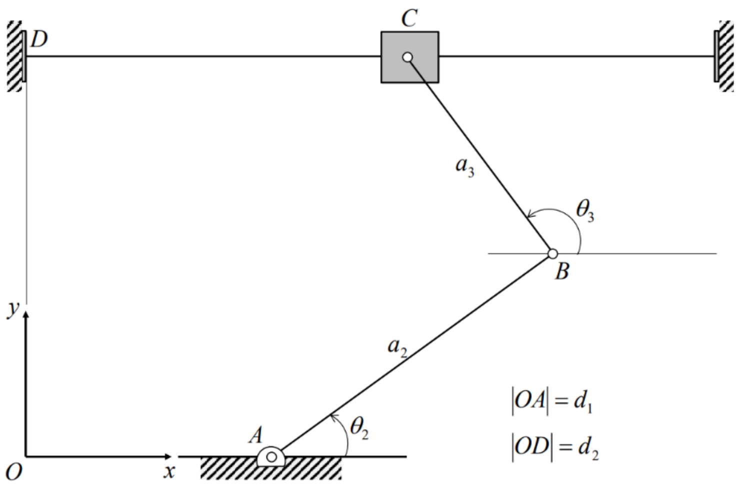

Fig 3.2.5. Robot Arm Free Body Diagram

For the given system loop closure equation can be given as:

$$\overrightarrow{OA} + \overrightarrow{AB} + \overrightarrow{BC} = \overrightarrow{OD} + \overrightarrow{DC} \tag{31}$$

$$d_1 + a_2 e^{i\theta_2} + a_3 e^{i\theta_3} = d_2 i + x_c \tag{32}$$

Direct kinematic equations for the position that finding x_c in terms of θ_2 while eliminating θ_3 for two possible trajectories is given below:

$$a_3 e^{i\theta_3} = d_2 i + x_c - d_1 - a_2 e^{i\theta_2} \quad (33)$$

$$a_3 e^{-i\theta_3} = -d_2 i + x_c - d_1 - a_2 e^{-i\theta_2} \quad (34)$$

For elimination, conjugates of the terms are multiplied below:

$$\begin{aligned} &a_2^2 + 2\cos(\theta_2)\, a_2 d_1 - 2\sin(\theta_2)\, a_2 d_2 \\ &-2cos(\theta_2) a_2 x_c + d_1^2 - 2 d_1 x_c + d_2^2 + x_c^2 = a_3^2 \end{aligned} \quad (35)$$

In order to solve the equation (36) for x_c, the equation can be re-written in the form:

$$Ax^2 + Bx + C = 0$$

Where,

$$A = 1,$$
$$B = -2(d_1 + a_2 cos(\theta_2))$$
$$C = a_2^2 + d_1^2 + d_2^2 - a_3^2 + 2a_2 d_1 cos(\theta_2) - 2a_2 d_2 sin(\theta_2)$$

Finally two different x_c Values are obtained as the roots of the rearranged equation:

$$x_{c,1} = \frac{-B + \sqrt{B^2 - 4AC}}{2A}$$

And,

$$x_{c,2} = \frac{-B - \sqrt{B^2 - 4AC}}{2A}$$

For making x_c real, $x_{c,2}$ is selected.

Direct kinematic equations for the position that finding x_c in terms of θ_3 while eliminating θ_2 for two possible trajectories given below:

$$a_3 e^{-i\theta_3} = -d_2 i + x_c - d_1 - a_2 e^{-i\theta_2} \quad (36)$$

For elimination, conjugates of the terms are multiplied below:

$$a_3^2 + 2\cos(\theta_2)\,a_3 d_1 - 2\sin(\theta_2)\,a_3 d_2$$
$$-2cos(\theta_2)a_3x_c + d_1^2 - 2d_1x_c + d_2^2 + x_c^2 = a_2^2 \qquad (37)$$

Equation (37) is solved by half tangent transformation as follows:

$$0 = K_1 + K_2cos(\theta_3) + K_3sin(\theta_3) \qquad (38)$$

$$0 = (K_1 - K_2)x^2 + (2K_3)x + (K_1 + K_2) \qquad (39)$$

$$A = K_1 - K_2; \quad B = 2K_3; \quad C = K_1 + K_2$$

And $x = \frac{-B\mp\sqrt{B^2-4AC}}{2A}$ and $x = tan\left(\frac{\theta_3}{2}\right)$

After the rearrangements, K values become as follows:

$$K_1 = -a_2^2 + a_3^2 + d_1^2 + d_2^2 + x_c^2 - 2d_1x_c$$
$$K_2 = 2a_3d_1 - 2a_3x_c$$
$$K_3 = -2a_3d_2$$

Finally, two different x_c Values are obtained as the roots of the rearranged equation:

$$\theta_{3,2} = 2arctan\left(\frac{-B + \sqrt{B^2 - 4AC}}{2A}\right)$$

And,

$$\theta_{3,2} = 2arctan\left(\frac{-B - \sqrt{B^2 - 4AC}}{2A}\right)$$

For making θ_3 real number, $\theta_{3,1}$ is selected.

Inverse kinematic equations can be reached as follows:

Finding θ_2 in terms of x_c while eliminating θ_3.

Rearranging equation (36)

$$(2a_2d_1 - 2a_2x_c)\cos(\theta_2) - (2a_2d_2)\sin(\theta_2)$$
$$+a_2^2 + d_1^2 + d_2^2 + x_c^2 - 2d_1x_c - a_3^2 = 0 \qquad (40)$$

K values become:

$$K_1 = +a_2^2 + d_1^2 + d_2^2 + x_c^2 - 2d_1x_c - a_3^2$$
$$K_2 = 2a_2d_1 - 2a_2x_c$$
$$K_3 = 2a_2d_2$$

Finally, two different θ_2 values are obtained as the roots of the rearranged equation:

$$\theta_{2,1} = 2arctan\left(\frac{-B + \sqrt{B^2 - 4AC}}{2A}\right)$$

And,

$$\theta_{2,2} = 2arctan\left(\frac{-B - \sqrt{B^2 - 4AC}}{2A}\right)$$

$\theta_{2,2}$ is selected regarding elbow position of robot arm.

A Maxon EC-max motor with a built in encoder used as an actuator for robot arm, solving inverse and forward kinematics each time. Robot position and reference position minimized using a PID controller, minimizing error between reference position inverse kinematics and motor's encoder.

Communication between the set-up and the software is provided by a National Instrument PCI Data Acquisition Board. As a software medium, Simulink Desktop Real-Time is utilized, and with its built-in features, the PCI board is introduced to the system. The board uses an external terminal for communication with the hardware.

3.3 Virtual Player Design

A single virtual player model is developed for VE and PE experimental rigs due to the highly adaptable nature of CPG proposed in [13] to any given signal. On VE, two CPGs with six-sub oscillators, one having exit from synchrony term [14] and mimicking human joystick inputs while the other learns the pre-recorded IMS time series. On the other hand, PE virtual player has the same build, except this time virtual player CPG trained with human position input on the rails. Later improvising, CPG architecture is implemented in the robot arm to create a triad improvisation.

Improvisation or follower CPG Model:

$$F_I(t) = x_{co} + f(t) \quad or \quad F_I(t) = x_{co} \tag{41}$$

$$\dot{x}_i = \gamma(\mu - r_i^2)x_i - \omega_i y_i + \epsilon F(t) + \tau \sin(\theta_i - \phi_i) \tag{42}$$

$$\dot{y}_i = \gamma(\mu - r_i^2)y_i + \omega_i x_i \tag{43}$$

$$\dot{\omega}_i = -\epsilon F(t) \frac{y_i}{r_i} \tag{44}$$

$$\dot{\alpha}_i = \eta x_i F(t) \tag{45}$$

$$\dot{\phi}_i = \sin\left(\frac{\omega_i}{\omega_0}\theta_0 - \theta_i - \phi_i\right) \tag{46}$$

$$\theta_i = \mathrm{sgn}(x_i)\cos^{-1}\left(-\frac{y_i}{r_i}\right) \tag{47}$$

$$F_I(t) = P_{\mathrm{teach}}(t) - Q_{\mathrm{learned}}(t) \tag{48}$$

$$Q_{\mathrm{learned}}(t) = \sum_{i=0}^{N} \alpha_i x_i \tag{49}$$

$$r = \sqrt{x^2 + y^2} \tag{50}$$

From Chapter 2 Eqn. (6) $f(t) = -nf_i + \beta_i \frac{v_j}{1+\frac{E}{E_0}} \xi_i$ Exit terms have been added as position drift to CPG input. x_{co} is the human position input. In the case of the following, the term $f(t)$ has been removed form $F_I(t)$, for virtual players, other parameters tuned as: $\alpha_i(0)$=$\phi_i(0)$=1, $y_i(0) = 0$, amplitude of oscillation $\mu = 1$, speed of recovery after perturbation $\gamma = 8$, coupling constant $\epsilon = 0.9$, strength between oscillator 0 and others τ=2 and the frequencies ω_i Distributed evenly from 6 to 70 between 6 sub-oscillators. For exit from synchrony term β_i=4, $n = 2$, $E_0 = 0.04$, $\tau = 1$ sec. and $\epsilon = 0.001$ parameters have tuned.

3.3.1 Virtual Environment Player Design

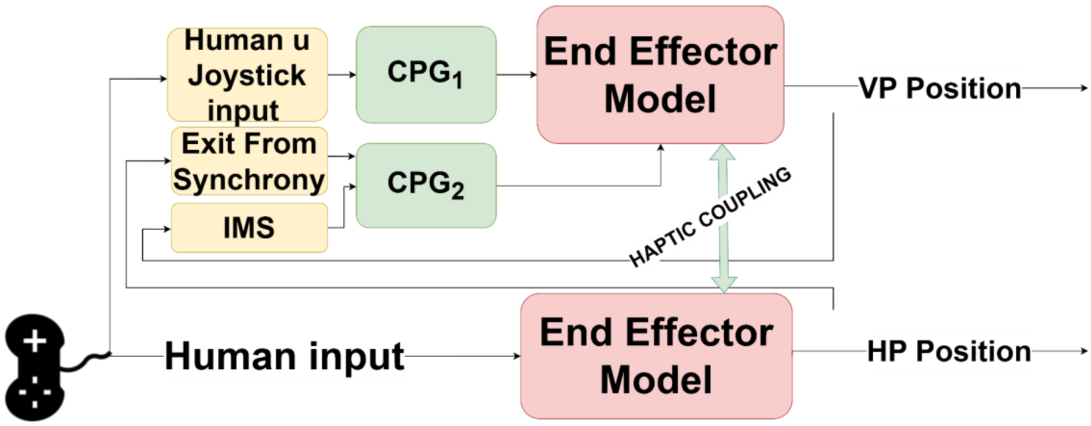

Fig 3.3.1.1 Virtual Environment VP Architecture

CPG_1 generated without the exit term acting as a follower for Human joystick inputs. CPG_2 generated with exit term coupling with the pre-recorded velocity time series of IMS. Since the human player plays with an end effector model, CPG architecture is built on playing with an end effector model.

CPG_2 output has been added to the end effector model as follows:

$$m\ddot{x}_{vp} + c\left(\dot{x}_{vp} + \dot{x}_{IMS}\right) = u - F_h \tag{51}$$

Where the $F_h = k(x_{VP} - x_{HP})$ Representing virtual haptic force. $\dot{x}_{IMS}$ is generated by CPG_2 with the exit term and u input generated by CPG_2. For human end effector model with virtual spring is defined as follows:

$$m\ddot{x}_{HP} + c\dot{x}_{HP} = u + F_h \tag{52}$$

3.3.2 Physical Environment Player Design

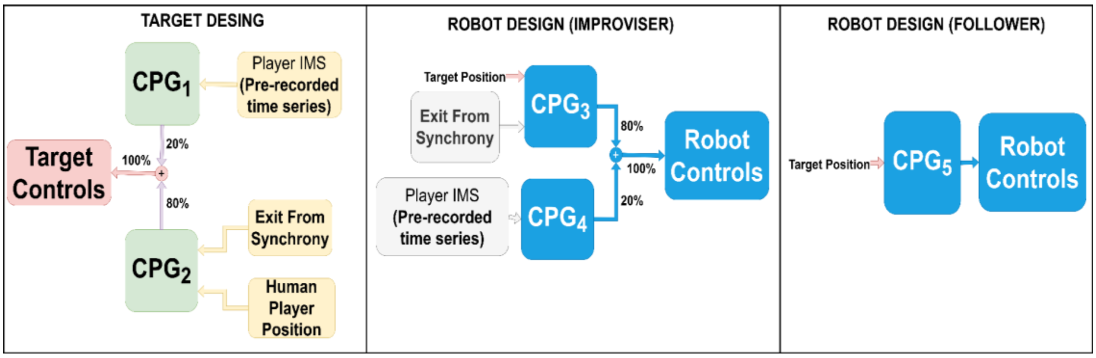

Fig 3.3.2.1 PE Virtual player design

Fig 3.3.2.1 shows a single mode of proposed virtual player designs; three distinct types of virtual agent designs utilized for further proposed experimental designs. Target improvises regardless of experimental scenarios that will be discussed in Chapter 4. Here CPG_1 learns human player pre-recorded IMS time series and CPG_2 learns human player movements with exit form synchrony term acting as a position drift when the velocity errors are small. For full motion, 20% of CPG_1 and 80% of CPG_2 have merged. Robot arm has two different roles as improviser or follower in game modes. Robot improviser model is identical with target model except CPG_4 learns some other signature different than players. CPG_3 learns either Target or human position inputs with exit from synchrony term. For Robot Follower model it only contains CPG_5 where robot either follows human player or target with human like errors. The physical parameters of the robot arm are defined as $a_2 = 209\,mm$, a_3=259 mm, $d_1 = 54.8\,mm$ and $d_2 = 274.5\,mm$ from real-life measurements.

CHAPTER 4

EXPERIMENTS

This chapter represents experiment scenario architectures for both virtual and physical environments to challenge players. Scenario outputs will be discussed in chapter 5. VE experiments consist of three classical modes as “solo,” Human Player-Human Player,” and “Human Player-Virtual Player” rounds with two different sub-modes, where players haptically coupled and not. PE experiments are carried out to test different haptic interaction scenarios. 5 different scenarios are deployed as “solo round” where the players asked to create motion how they like. Second as “Target-Human Joint Improvisation (THJI),” where the player and target improvise without haptic coupling. “. The third is “Human Driven Haptics Joint Improvisation (HDHJI).” Where the robot arm follows human movements and interacts with the human player. The fourth is “Target Driven Haptics Joint Improvisation (TDHJI).” Where the robot arm follows the target’s movements and interacts with the human player, and finally, the fifth mode is called “Triad Joint Improvisation (TJI).” Where robot improvises with target interacting with a human player. Target both improvises with human player and robot.

4.1 Virtual Environment Experiments.

The experimental medium is arranged using MATLAB-Simulink using the Virtual Reality system toolbox. The system consists of two ball avatars on parallel axis with three different game modes arrangeable:

- Solo round
- HP-HP round with H+ or H-
- HP-VP round with H+ or H-

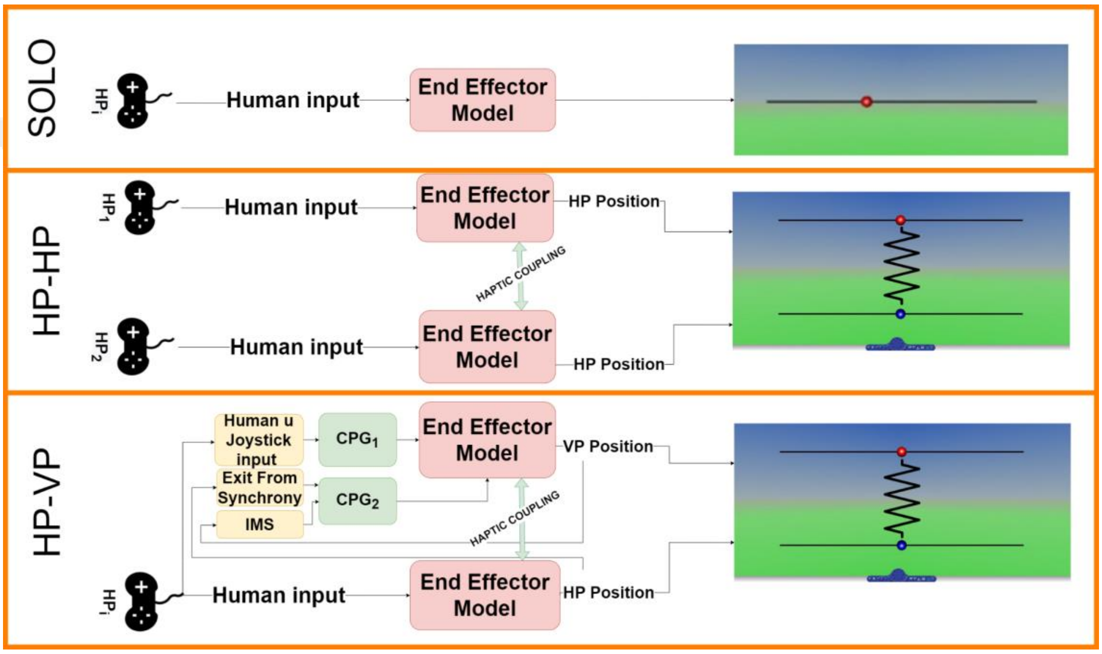

Fig 4.1.1 VE Experiment Modes

This experiment acted as a virtual agent verification; each player played three rounds in each mode, and every round played for 60 seconds. Each player played 15 rounds, including three solos, three HP-HP H+, three HP-HP H-, three HP-VP H+, and three HP-VP H-.

Fig 4.1.2 Dyad Playing HP-HP round

4.2 Physical Environment Experiments.

In this experiment, 20 people attended all scenarios:

- The age range of participants is between 20 and 30.
- Three solo rounds, each lasting 60 seconds, are played by every player.
- Three THJI rounds lasting 60 seconds each are played by every player.
- Three HDHJI rounds lasting 60 seconds each are played by every player.
- Three TDHJI rounds lasting 60 seconds each are played by every player.
- Three TJI rounds lasting 60 seconds each are played by every player.
- The human players could see the target and laser pointer mark easily.
- Solo, THJI, HDHJI, TDHJI, and TJI rounds are played consecutively by finishing each scenario three by three.

4.2.1 Solo Rounds

On solo rounds, it has been asked players to create interesting motions and enjoy; only the human handle data input was open all the time, recording patterns players had created. Later, positions recorded are converted into velocity time series to implement in virtual agent architecture.

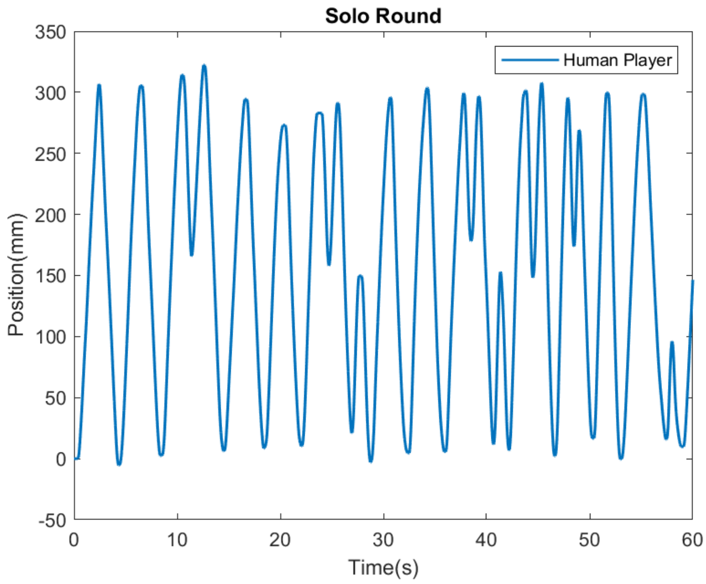

Fig 4.2.1.1 Solo Round Data Recording

Fig 4.2.1.1 shows an example of solo round data recording; players moved how they liked and created motion patterns how they liked. Later solo positions converted into velocity time series to compute individual motor signatures and train virtual agents.

4.2.2 Target Human Joint Improvisation (THJI)

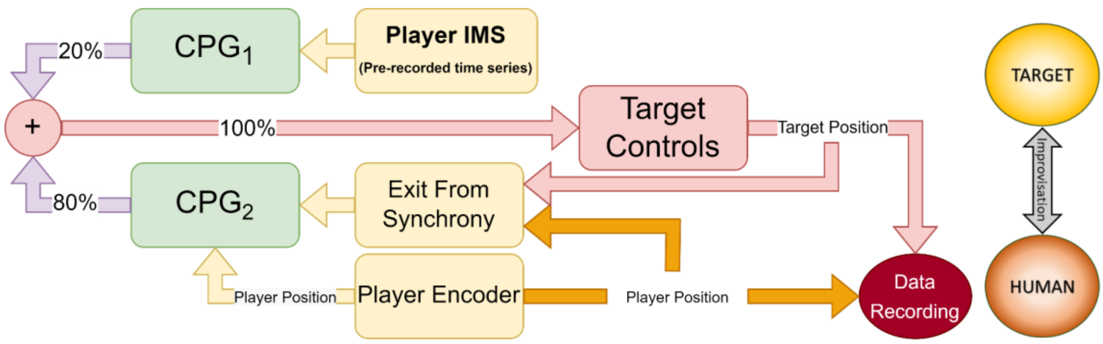

Fig 4.2.2.1 THJI Game Mode

THJI game mode is employed as a control group to study human movement characteristics without haptic feedback. Where players' specific solo round velocity time series fed through CPG_1, and CPG_2 fed with human position inputs during the game with a coupled exit from synchrony term. The robot arm was offline and standing aside during game rounds.

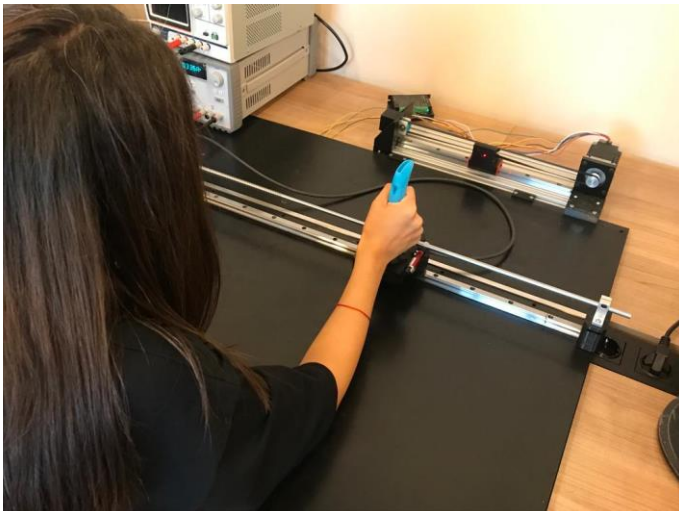

Fig 4.2.2.2 THJI During Game Round

With similar fashion target movements generated form 20% of CPG_1 and 80% of CPG_2. After three consecutive game rounds, it has asked players to move back to prepare for the next round Human Driven Haptics Joint Improvisation (HDHJI).

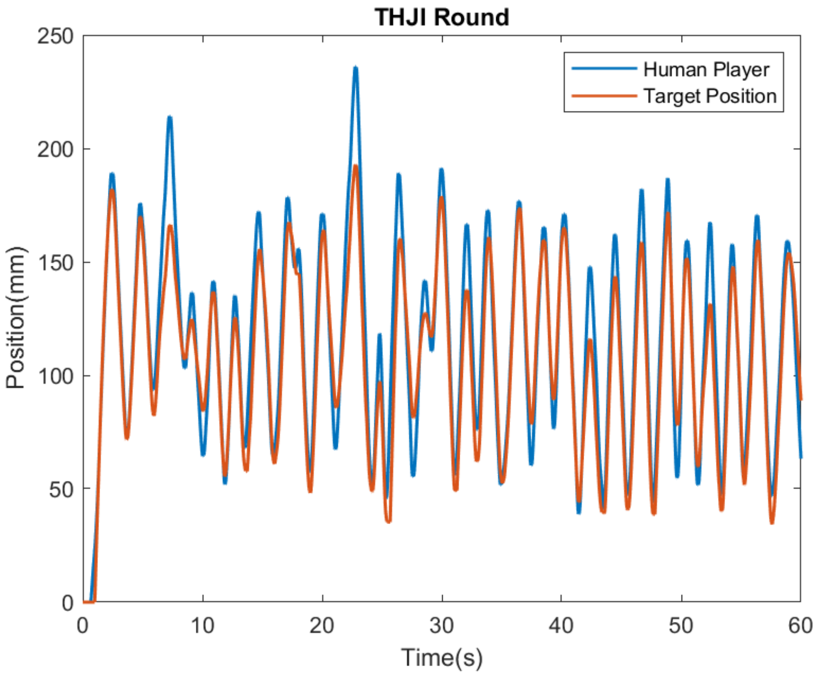

Fig 4.2.2.3 THJI Round Data Recording

Fig 4.2.2.3 shows an example of THJI round data recording; players improvise freely with the target. Robot arm is offline throughout the game rounds.

4.2.3 Human-Driven Haptic Joint Improvisation (HDHJI)

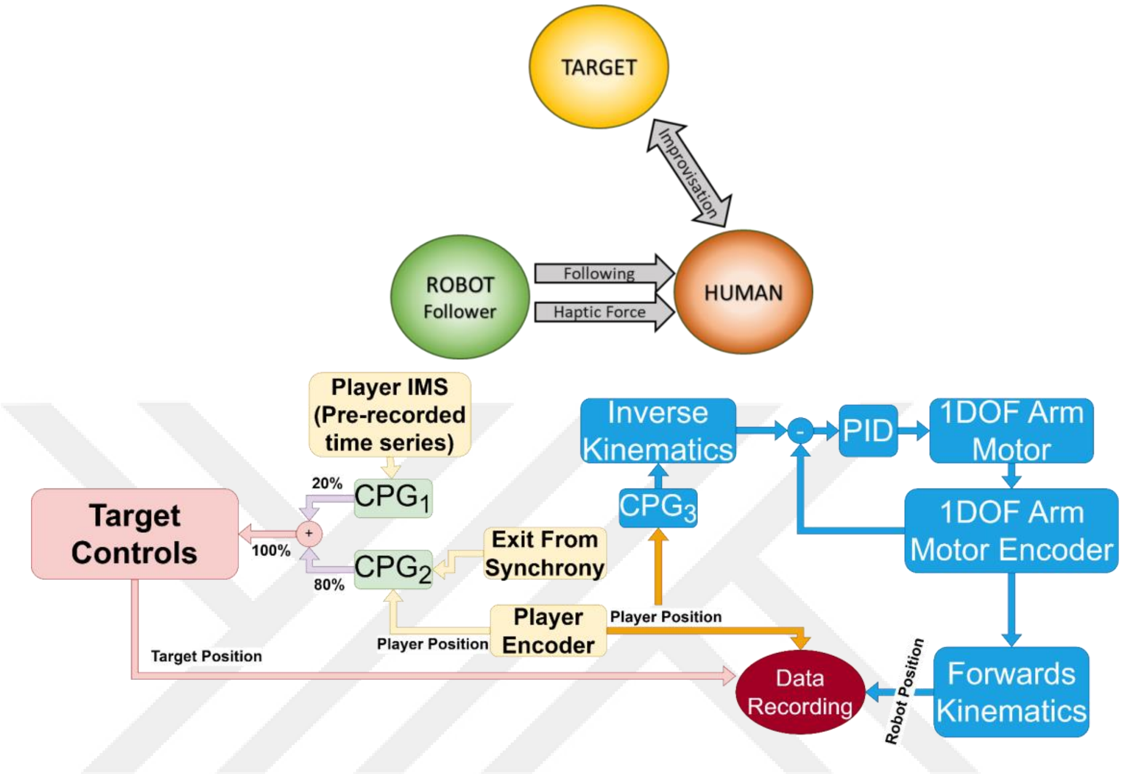

Fig 4.2.3.1 HDHJI Game Mode

HDHJI game mode is employed to create a variety of haptic interaction forces in means of complexity. The robot arm follows and interacts with the human co-actor while the human co-actor improvises with the target. CPG_1, CPG_2 have the same dynamics described in THJI and CPG_3 acts as a follower of human position input. The robot arm had driven with feeding human position to inverse kinematics to get θ_2 later corresponding θ_2 fed through forward kinematics to record end effectors' position for related formulation; please see Section 3.2.

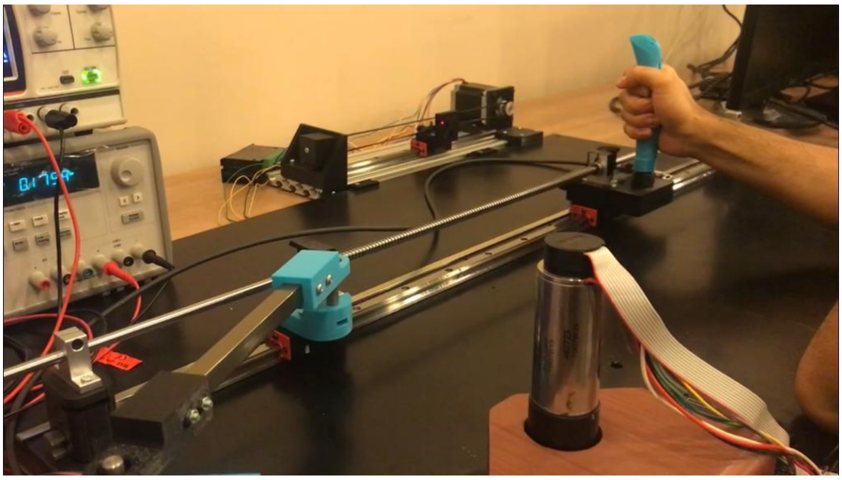

Fig 4.2.3.2 HDHJI During Game Round

Fig 4.2.3.2 shows the play stile during HDHJI rounds, robot arm follows human position inputs. The same kind of stile applies for all game modes except THJI.

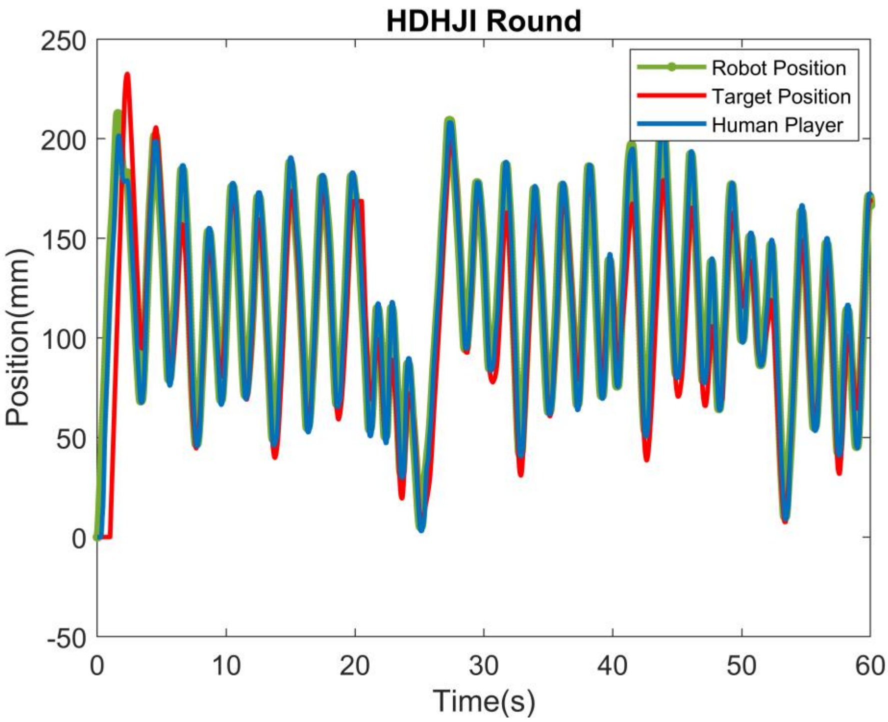

Fig 4.2.3.3 HDHJI Example Game Round

Fig 4.2.3.3 shows an example round of HDHJI green dotted lines are the robot's position, and it can clearly see that robot follows the human player during the game round with human-like errors.

4.2.4 Target-Driven Haptic Joint Improvisation (TDHJI)

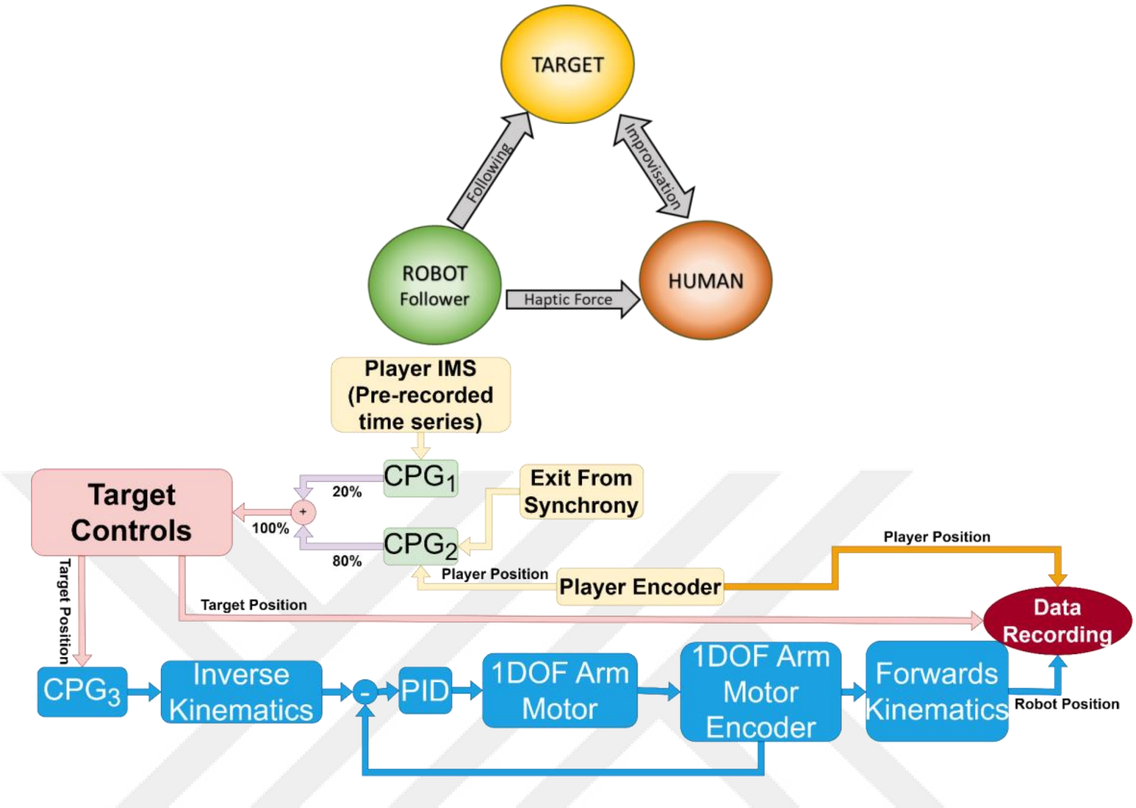

Fig 4.2.4.1 TDHJI Game Mode

TDHJI game mode is employed to create a variety of haptic interaction forces in means of complexity. The robot arm follows the target interacting with the human co-actor while the human co-actor improvises with the target. TDHJI has only one difference from HDHJI, which is the robot CPG_3 follows target position instead of human encoder inputs.

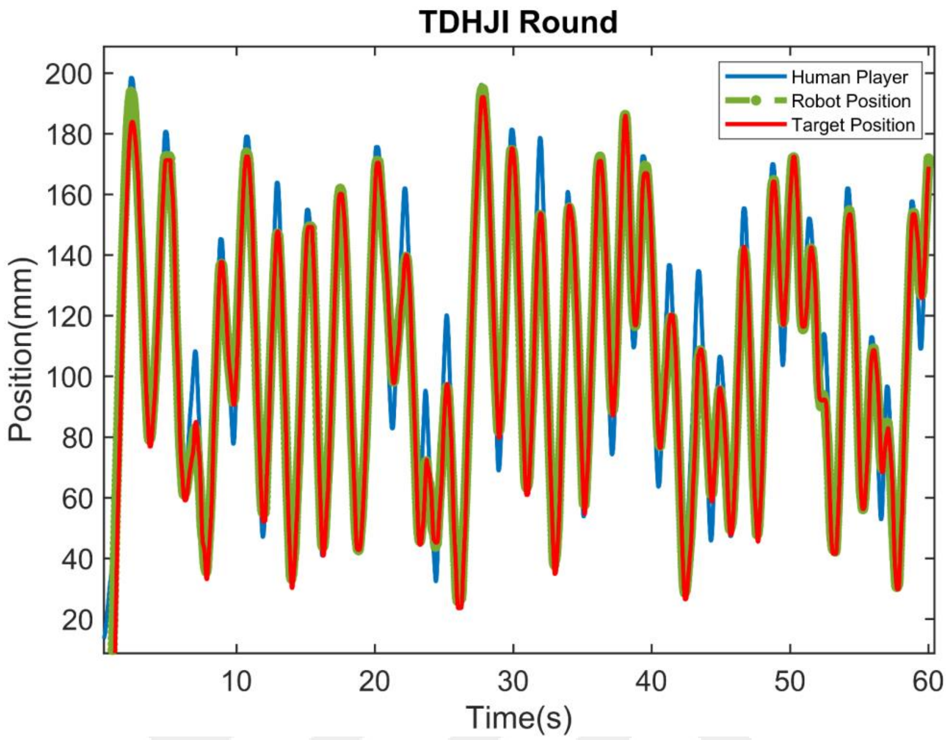

Fig 4.2.4.2 TDHJI Example Game Round

Fig 4.2.4.2. shows an example round of TDHJI, and green highlighted lines show the robot position following the target position with human-like errors.

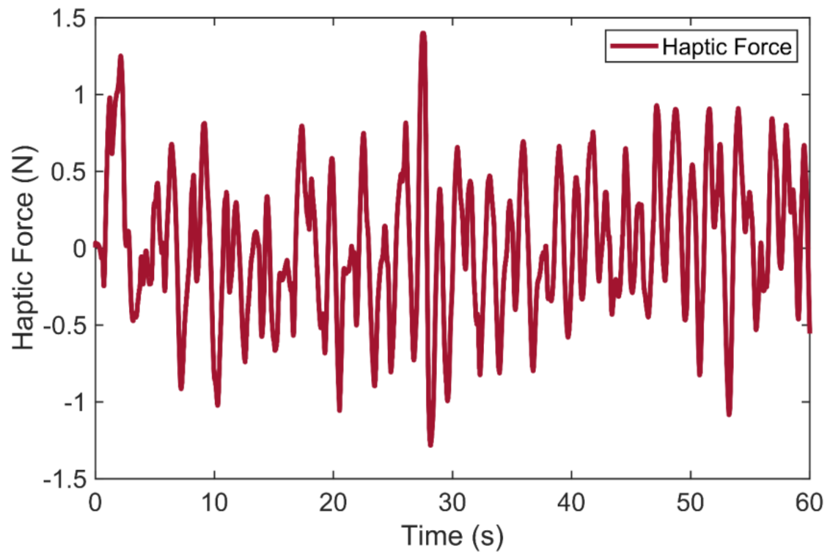

Fig 4.2.4.3 Example TDHJI Haptic Force Graph

Fig 4.2.4.3 shows an example of haptic force generated during the TDHJI round. All data points are calculated with a known spring stiffness value k=0.026 N/mm.

4.2.5 Triad Joint Improvisation (TJI)

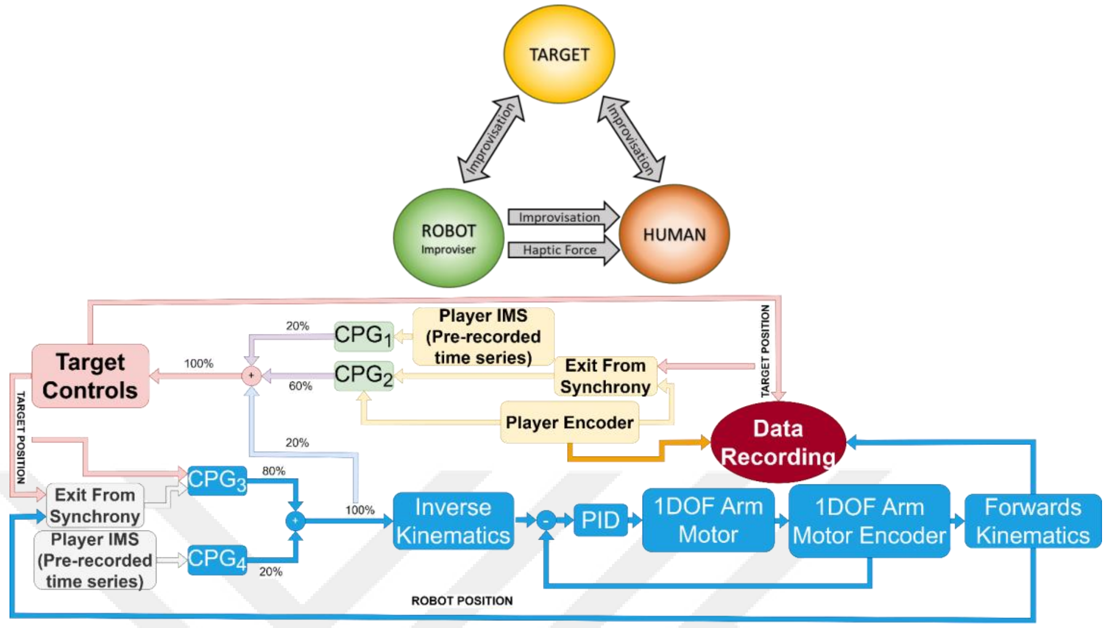

Fig 4.2.5.1 TJI Game Mode

Fig 4.2.5.1 shows the triad joint improvisation architecture; an additional CPG has been added to robot dynamics. Here target acquires position input from both human and robot acting in a way that improvises with both human co-actor and robot. Target controls get it's position input 20% from the robot, 60% from the human co-actor, and 20% from pre-recorded IMS time series. Those values adjusted from real-life experience to build a game playable for human co-actor. On the other hand, target movements generated 80% of target movements, including exit from synchrony term between target and robot, and 20% from pre-recorded IMS time series of a fellow lab mate giving a static personality to the robot arm.

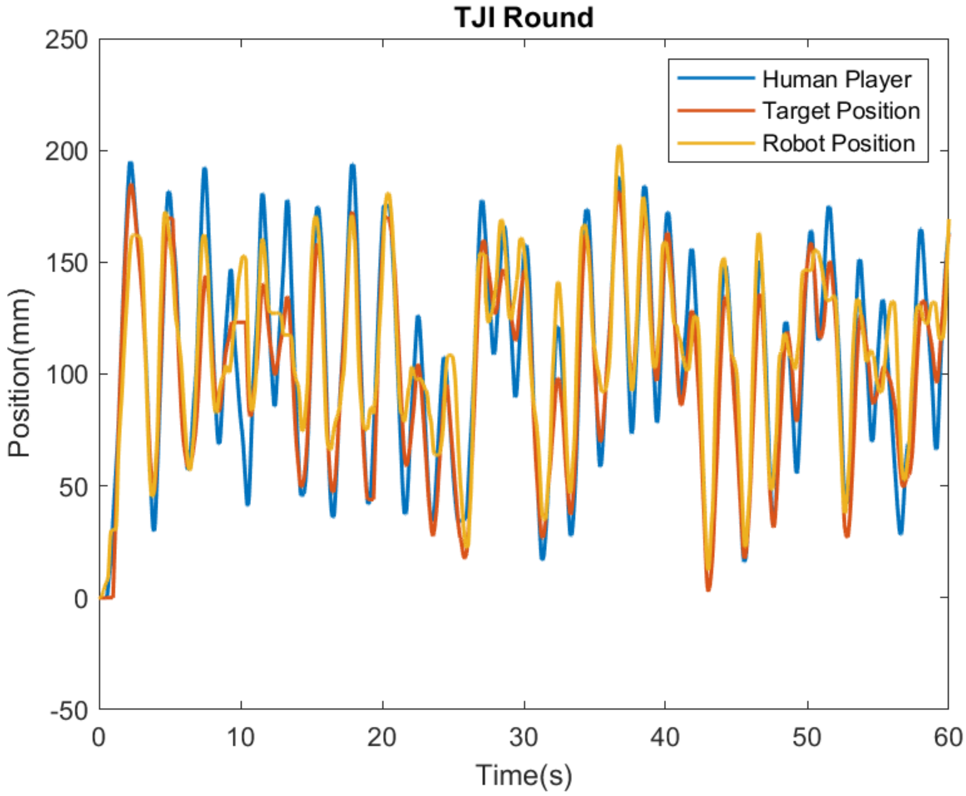

Fig 4.2.5.2 TJI Round Data Recording

Fig 4.2.5.2 shows a typical round of improvising as a triad; it can clearly be seen that every co-actor is moving in their own way but trying to synchronize. It's not asked for players to pay attention to robot movements, but human, robot, and target movements coupled with the proposed architecture.

CHAPTER 5

DATA AND EVALUATION OF METRICS

In chapter 2, metrics used in the literature are defined. This study utilizes the performance of co-actors measured using circular variance (CV), earth mover distance (EMD), entropy, and RMS of position error. Instead of using the CC metric in the literature, this study utilizes a new way to compute CC periods from relative phase signals; also, this new approach helped to define leaders during the game.

5.1 Relative Phase

In order to distinguish the leaders in the mirror game relative phase between the players will be calculated. All position differences mapped between 2π and -2π Where Hilbert Transform H(t) of x(t) serves as the imaginary part of an analytical signal, x_1 and x_2 denote the players' positions, the phase angle at time t_i can be calculated by:

$$\phi(t_i) = arctan\left(\frac{H_{1,2}(t_i)}{x_{1,2}(t_i)}\right) \tag{53}$$

The relative phase between players can be calculated by:

$$RP = \phi_1(t_i) - \phi_2(t_i) = arctan\left(\frac{H_1(t_i)x_2(t_i) - H_2(t_i)x_1(t_i)}{x_1(t_i)x_2(t_i) + H_1(t_i)H_2(t_i)}\right) \tag{54}$$

where $H_1(t)$ and $H_2(t)$ Denote the Hilbert transform of each signal, respectively [60].

5.2 Circular Variance (CV)

Since the 0-phase difference means players standing in the same overall position performance quantified using circular variance (CV) with the equation [55]:

$$\mathrm{CV} = \left\| \frac{1}{\mathrm{k}} \sum_{\mathrm{j}=1}^{k} \exp\left(\mathrm{i}\Delta\phi_{\mathrm{j}}\right) \right\| \quad \in [0,1] \tag{55}$$

where $\Delta\phi_j$ is the relative phase between the leader and follower, and k represents the number of time steps. Where the cumulative result varies between 0 to 1, 1 means full synchronization, and 0 means no synchronization.

5.3 Co-Confident Motion

Prior research showed that, if the distance between peak events are smaller than 0.3s[11] and normalized velocity error between velocity segments are smaller than 0.95[43] those periods of movements named as CC motion with averaged 3 to 14% on a game mode. Regarding that information a new approach have developed from relative phase.

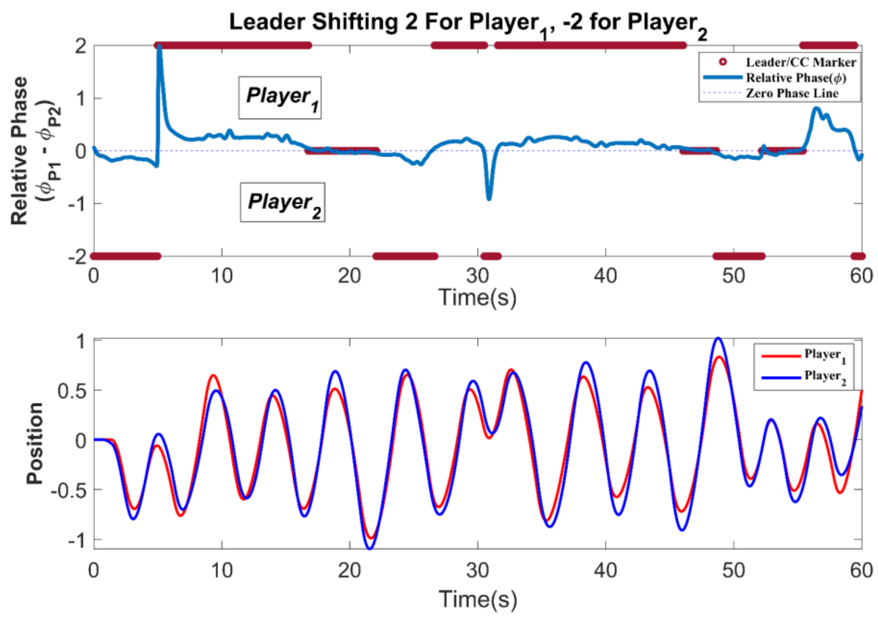

Fig 5.3.1. Position of players and change of leadership via relative phase during game round.

In this work, if the phase difference is smaller than 0.06 *rad* for more than 1 second, those movements named CC motion, regions smaller than 1 second, removed from CC zones and added to the previous leader.

The bottom graph shows a typical joint improvisation round from a VE Experiment, and the top graph shows the relative phase difference throughout the game round. Since the algorithm extracts Player 1 phase from the Player 2 phases, on phase graph values smaller than 0 show the player 2's leading region; with that kind of approach for that specific round leadership and CC motion states calculated as: CC=12.26%, Player 1= 53.52% and Player 2 = 34.21%.

The same kind of approach is used for both VE and PE Experiments.

5.4 Position Temporal Correspondence (RMS)

The normalized position error between the leader and follower is defined by the root mean square (RMS) [56]. It refers to how well they coordinated their movements throughout the game.

$$\mathrm{RMS} = \frac{1}{M}\sqrt{\frac{1}{n}\sum_{k=1}^{n}(x_{1,k} - x_{2,k})^2} \tag{56}$$

where M stands for the set of permitted locations, n for sample steps number throughout the simulation, and $x_{1,k}$ and $x_{2,k}$ refer for co-actors positions.

5.5 The Earth Mover's Distance (EMD)

To find IMS and evaluate the position error between VP and HP, the Earth Mover's Distance is calculated as follows [17]:

$$\mathrm{EMD} = \int_z \left|\mathrm{CDF}_{p_1}(z) - \mathrm{CDF}_{p_2}(z)\right| dz \tag{57}$$

where PDF_1 and PDF_2 represent the velocity PDF for HP and VP, and their cumulative distribution is shown as CDF_1 and CDF_2. This measurement was performed after the process of the game rounds EMD was calculated on all combinations meaning Humans' solo round signature vs. in-game signature, the same kind of process applied to virtual players as well to denote their in-game adaptation levels.

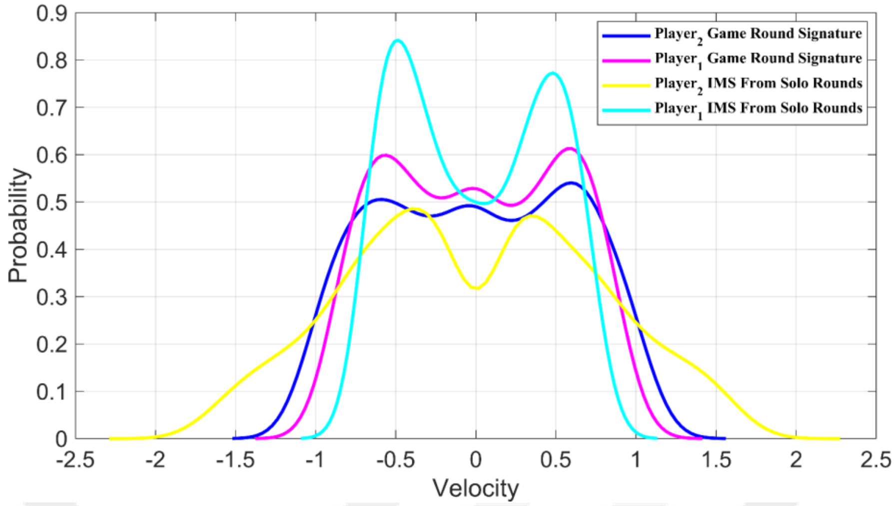

Fig 5.5.1. Example Individual Motor Signatures of Players

Fig 5.5.1 shows the Human signatures displayed in the game showcased in Fig 5.3.1 CC motion; distance between signatures could be defined as distances (EMD):

Table 5.1: Example EMD Distribution of Game Round

Motor signature		Interaction	
$\eta(\sigma_1, \mu_1)$	0.0095		
$\eta(\sigma_2, \mu_2)$	0.0251	$\eta(\mu_1, \mu_2)$	0.0035
$\eta(\sigma_1, \sigma_2)$	0.035		

Where $\eta(\sigma_1, \mu_1)$ Shows player 1's in-game and solo round signature distance (EMD), $\eta(\sigma_2, \mu_2)$ shows Player 2's solo round and in-game distance (EMD), $\eta(\sigma_1, \sigma_2)$ shows how close the co-actors' signatures and $\eta(\mu_1, \mu_2)$ shows in-game signature difference (EMD). Regarding the outputs of CC and EMD. Player 1 refused to change his/her own signature, which end up he is leading more in the game, and player 2 adapted his/her partner much more.

5.6 Shannon Entropy

Shannon Entropy represents the average level of uncertainty of random variables [59]. It shows which of the followers exhibit complex movements.

$$E = -\sum p(n) \log_2 p(n) \tag{58}$$

where p(n) corresponds to the probability associated to the occurrence of the event, n.

This metric will be used to quantify human robot and target movement entropies, effects of haptic interaction complexity will be discussed in Chapter 6.

CHAPTER 6

RESULTS AND DISCUSSION

This section aims to investigate the varying experiment scenarios in virtual and physical, mentioned in Chapter 4. Metrics displayed in Chapter 5 are employed for studying interaction dynamics with different meanings. The results are divided into two subsections for VE and PE.

6.1. Results and Discussion of Virtual Environment Experiments

- Human Player-Human Player Rounds

Table 6.1: HP_1-HP_2 Rounds Metric Outputs

HP_1- HP_2 H- Round 1				**HP_1- HP_2 H+ Round 1**			
Motor Signature		**Interaction**		**Motor Signature**		**Interaction**	
$\eta(\sigma_1,\mu_1)$	**0.04**			$\eta(\sigma_1,\mu_1)$	**0.042**		
$\eta(\sigma_2,\mu_2)$	**0.02**	$\eta(\mu_1,\mu_2)$	**0.003**	$\eta(\sigma_2,\mu_2)$	**0.0265**	$\eta(\mu_1,\mu_2)$	**0.0071**
$\eta(\sigma_1,\sigma_2)$	**0.0186**			$\eta(\sigma_1,\sigma_2)$	**0.0186**		
Stats	**HP_1**	**HP_2**	**CC**	**Stats**	**HP_1**	**HP_2**	**CC**
100%	**24.12%**	**66.90%**	**8.96%**	**100%**	**18.18%**	**73.99%**	**7.83%**
CV	**0.8265**			**CV**	**0.8854**		
HP_1- HP_2 H- Round 2				**HP_1- HP_2 H+ Round 2**			
Motor Signature		**Interaction**		**Motor Signature**		**Interaction**	
$\eta(\sigma_1,\mu_1)$	**0.034**			$\eta(\sigma_1,\mu_1)$	**0.0324**		
$\eta(\sigma_2,\mu_2)$	**0.027**	$\eta(\mu_1,\mu_2)$	**0.0055**	$\eta(\sigma_2,\mu_2)$	**0.0274**	$\eta(\mu_1,\mu_2)$	**0.0083**
$\eta(\sigma_1,\sigma_2)$	**0.0186**			$\eta(\sigma_1,\sigma_2)$	**0.0186**		
Stats	**HP_1**	**HP_2**	**CC**	**Stats**	**HP_1**	**HP_2**	**CC**
100%	**21.51%**	**70.70%**	**7.70%**	**100%**	**12.8%**	**70.22%**	**16.98%**
CV	**0.9084**			**CV**	**0.9173**		
HP_1- HP_2 H- Round 3				**HP_1- HP_2 H+ Round 3**			
Motor Signature		**Interaction**		**Motor Signature**		**Interaction**	
$\eta(\sigma_1,\mu_1)$	**0.0343**			$\eta(\sigma_1,\mu_1)$	**0.0349**		
$\eta(\sigma_2,\mu_2)$	**0.0273**	$\eta(\mu_1,\mu_2)$	**0.0066**	$\eta(\sigma_2,\mu_2)$	**0.0273**	$\eta(\mu_1,\mu_2)$	**0.0057**
$\eta(\sigma_1,\sigma_2)$	**0.0186**			$\eta(\sigma_1,\sigma_2)$	**0.0186**		
Stats	**HP_1**	**HP_2**	**CC**	**Stats**	**HP_1**	**HP_2**	**CC**
100%	**11.79%**	**76.48%**	**11.71%**	**100%**	**12.4%**	**71.05%**	**16.55%**
CV	**0.9746**			**CV**	**0.9841**		

According to Table 6.1 data, player 1 was better at adapting to the opposing side. Player 2 took on more leadership roles throughout the game rounds because of his/her refusal to adapt. Player 1 benefited the most from haptic coupling rounds because their co-confident motion states with their counterpart were higher. In other words, the H+ condition has improved Player 1’s ability to synchronize and adapt his/her own motor signature.

- Human Player 1-Virtual Player Rounds

Table 6.2: HP_1-VP Rounds Metric Outputs

HP_1-VP H- Round 1				**HP_1-VP H+ Round 1**			
Motor Signature		**Interaction**		**Motor Signature**		**Interaction**	
$\eta(\sigma_1,\mu_1)$	**0.0209**			$\eta(\sigma_1,\mu_1)$	**0.0224**		
$\eta(\sigma_2,\mu_2)$	**0.0207**	$\eta(\mu_1,\mu_2)$	**0.003**	$\eta(\sigma_2,\mu_2)$	**0.0237**	$\eta(\mu_1,\mu_2)$	**0.0092**
$\eta(\sigma_1,\sigma_2)$	**0.0357**			$\eta(\sigma_1,\sigma_2)$	**0.0357**		
Stats	**HP_1**	**VP**	**CC**	**Stats**	**HP_1**	**VP**	**CC**
100%	**33.41%**	**57.59%**	**9.00%**	**100%**	**16.41%**	**62.21%**	**21.38%**
CV	**0.9841**			**CV**	**0.9788**		
HP_1-VP H- Round 2				**HP_1-VP H+ Round 2**			
Motor Signature		**Interaction**		**Motor Signature**		**Interaction**	
$\eta(\sigma_1,\mu_1)$	**0.0227**			$\eta(\sigma_1,\mu_1)$	**0.0269**		
$\eta(\sigma_2,\mu_2)$	**0.0153**	$\eta(\mu_1,\mu_2)$	**0.0019**	$\eta(\sigma_2,\mu_2)$	**0.0117**	$\eta(\mu_1,\mu_2)$	**0.0035**
$\eta(\sigma_1,\sigma_2)$	**0.0357**			$\eta(\sigma_1,\sigma_2)$	**0.0357**		
Stats	**HP_1**	**VP**	**CC**	**Stats**	**HP_1**	**VP**	**CC**
100%	**43.14%**	**35.58%**	**21.28%**	**100%**	**37.21%**	**53.52%**	**9.27%**
CV	**0.9831**			**CV**	**0.9282**		
HP_1-VP H- Round 3				**HP_1-VP H+ Round 3**			
Motor Signature		**Interaction**		**Motor Signature**		**Interaction**	
$\eta(\sigma_1,\mu_1)$	**0.0232**			$\eta(\sigma_1,\mu_1)$	**0.0222**		
$\eta(\sigma_2,\mu_2)$	**0.0213**	$\eta(\mu_1,\mu_2)$	**0.003**	$\eta(\sigma_2,\mu_2)$	**0.0262**	$\eta(\mu_1,\mu_2)$	**0.0104**
$\eta(\sigma_1,\sigma_2)$	**0.0357**			$\eta(\sigma_1,\sigma_2)$	**0.0357**		
Stats	**HP_1**	**VP**	**CC**	**Stats**	**HP_1**	**VP**	**CC**
100%	**45.44%**	**36.59%**	**17.96%**	**100%**	**9.90%**	**81.25%**	**8.85%**
CV	**0.8265**			**CV**	**0.9841**		

The proposed Virtual Player exhibits similar outcomes to human players in terms of CV and leadership taking; VP can adapt its motor signature to human counterpart; VP not only exhibits leadership qualities but also follows and permits human counterpart to have fun and learn about the game.

- Human Player 2-Virtual Player Rounds

Table 6.3: HP_2-VP Rounds Metric Outputs

HP_2-VP H- Round 1				HP_2-VP H+ Round 1			
Motor Signature		Interaction		Motor Signature		Interaction	
$\eta(\sigma_1,\mu_1)$	0.0436			$\eta(\sigma_1,\mu_1)$	0.0505		
$\eta(\sigma_2,\mu_2)$	0.3064	$\eta(\mu_1,\mu_2)$	0.0018	$\eta(\sigma_2,\mu_2)$	0.0296	$\eta(\mu_1,\mu_2)$	0.0016
$\eta(\sigma_1,\sigma_2)$	0.2318			$\eta(\sigma_1,\sigma_2)$	0.2318		
Stats	HP_2	VP	CC	Stats	HP_2	VP	CC
100%	28.37%	63.3%	8.31%	100%	51.52%	38.44%	10.03%
CV	0.8974			CV	0.9099		
HP_2-VP H- Round 2				**HP_2-VP H+ Round 2**			
Motor Signature		Interaction		Motor Signature		Interaction	
$\eta(\sigma_1,\mu_1)$	0.0405			$\eta(\sigma_1,\mu_1)$	0.1834		
$\eta(\sigma_2,\mu_2)$	0.2931	$\eta(\mu_1,\mu_2)$	0.008	$\eta(\sigma_2,\mu_2)$	0.2861	$\eta(\mu_1,\mu_2)$	0.0061
$\eta(\sigma_1,\sigma_2)$	0.2318			$\eta(\sigma_1,\sigma_2)$	0.2318		
Stats	HP_2	VP	CC	Stats	HP_2	VP	CC
100%	35.39%	58.12%	6.48%	100%	49.08%	38.66%	12.26%
CV	0.9093			CV	0.9426		
HP_2-VP H- Round 3				**HP_2-VP H+ Round 3**			
Motor Signature		Interaction		Motor Signature		Interaction	
$\eta(\sigma_1,\mu_1)$	0.1869			$\eta(\sigma_1,\mu_1)$	0.1779		
$\eta(\sigma_2,\mu_2)$	0.2894	$\eta(\mu_1,\mu_2)$	0.0045	$\eta(\sigma_2,\mu_2)$	0.2879	$\eta(\mu_1,\mu_2)$	0.0091
$\eta(\sigma_1,\sigma_2)$	0.2318			$\eta(\sigma_1,\sigma_2)$	0.2318		
Stats	HP_2	VP	CC	Stats	HP_2	VP	CC
100%	40.66%	48.43%	10.91%	100%	54.02%	33.63%	12.35%
CV	0.9409			CV	0.9293		

HP2 showed more leading outputs when playing with a human player. However, while playing with the virtual player, in non-haptic rounds player showed a higher following pattern; after enabling haptic interaction player granted back his/her leadership back, and overall CC motion is increased. Since $\eta(\sigma_1,\sigma_2)$ virtual player IMS and human player IMS distance is greater than HP_1-VP rounds, HP_2 performed attenuated results in game performance compared to HP_1.

6.2 Results and Discussion of Physical Environment Experiments

This experiment is carried out to quantify different haptic interaction scenarios and study effects on human performance; therefore, starting with CV game performance over the game rounds is logical to build the right reasoning.

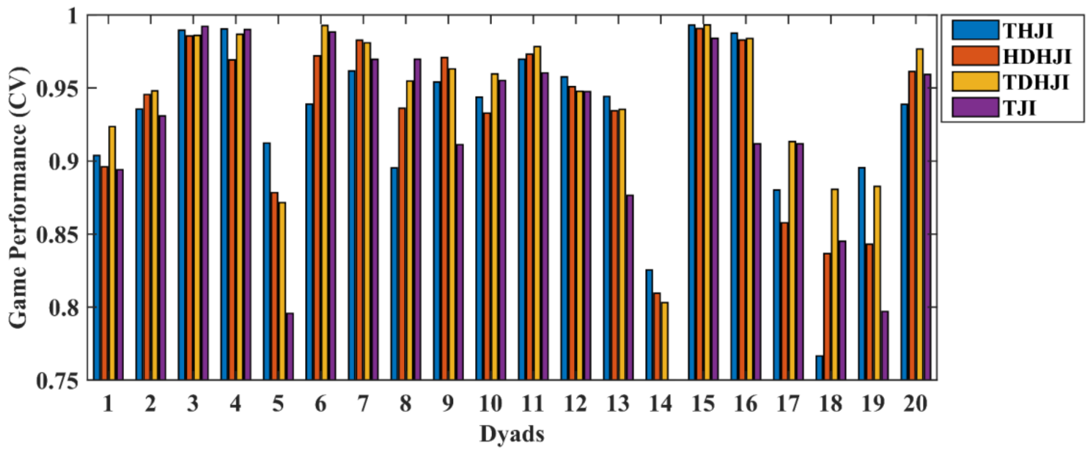

Fig 6.2.1. CV Game Performance Dyadic Average

Fig 6.2.1 shows the dyads' average game performance over four separate game rounds. It has been found that few players played the game in unexpected ways, such as making fast and jittery motions that made them hard to synchronize and play with the target; they acquired very poor results in means of CV and showed no progression with the haptic coupling enabled. Players had better performance on TDHJI rounds compared to other game modes. 70% of participants showed increased levels of synchronization on TDHJI rounds when compared to TJI (H-). 50% showed increased levels of synchronization compared to TJI(H-) rounds, and finally, on TJI rounds, players had poor game performance; only 40% of people showed increased levels of coordination, which may happen due to the complex dynamics of TJI where target did not fully improvise with the human players. Since the psychological status of players is unknown, it is not possible to group participants with known facts about their lives.

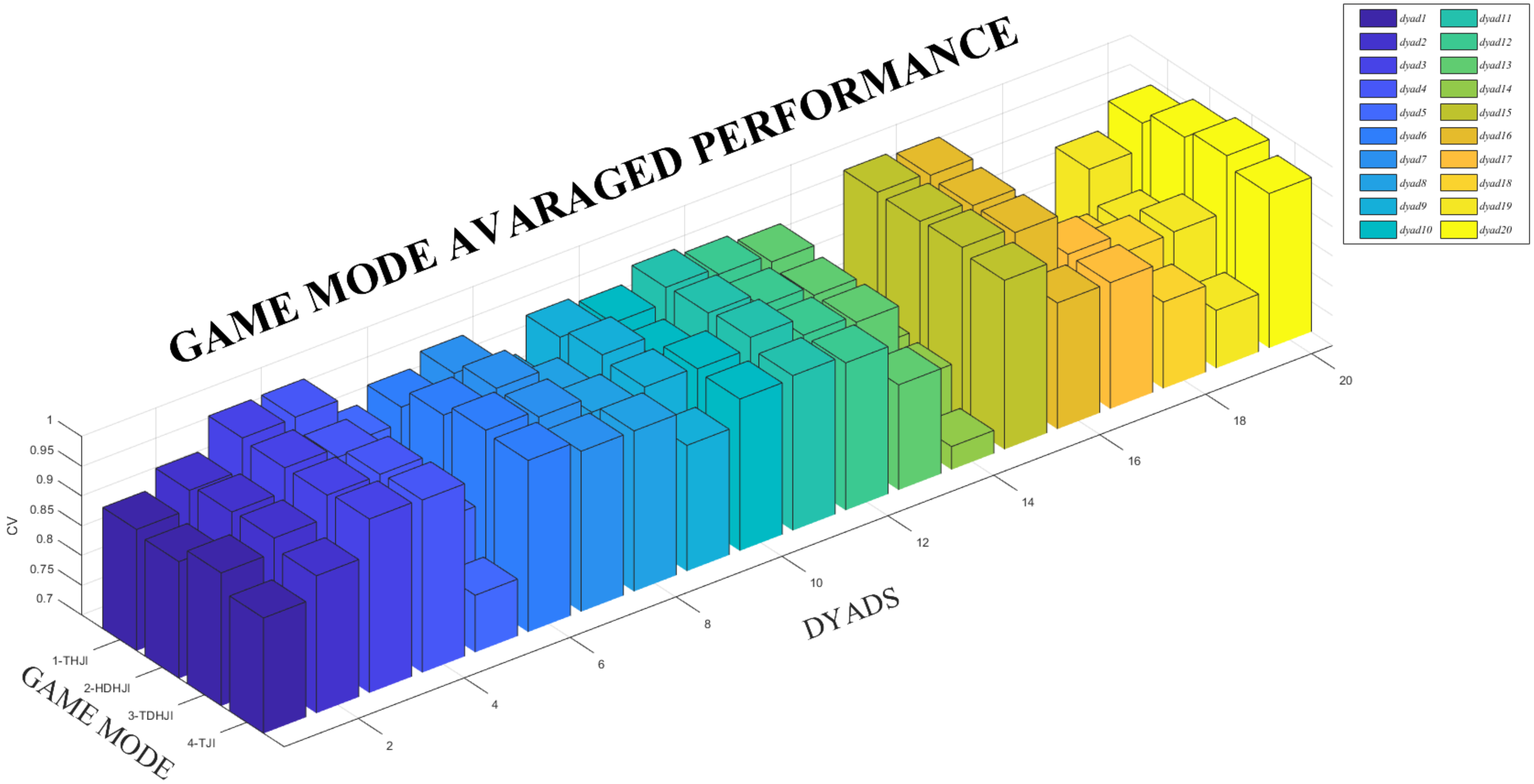

Fig 6.2.2. CV Game Performance Dyadic Average-2

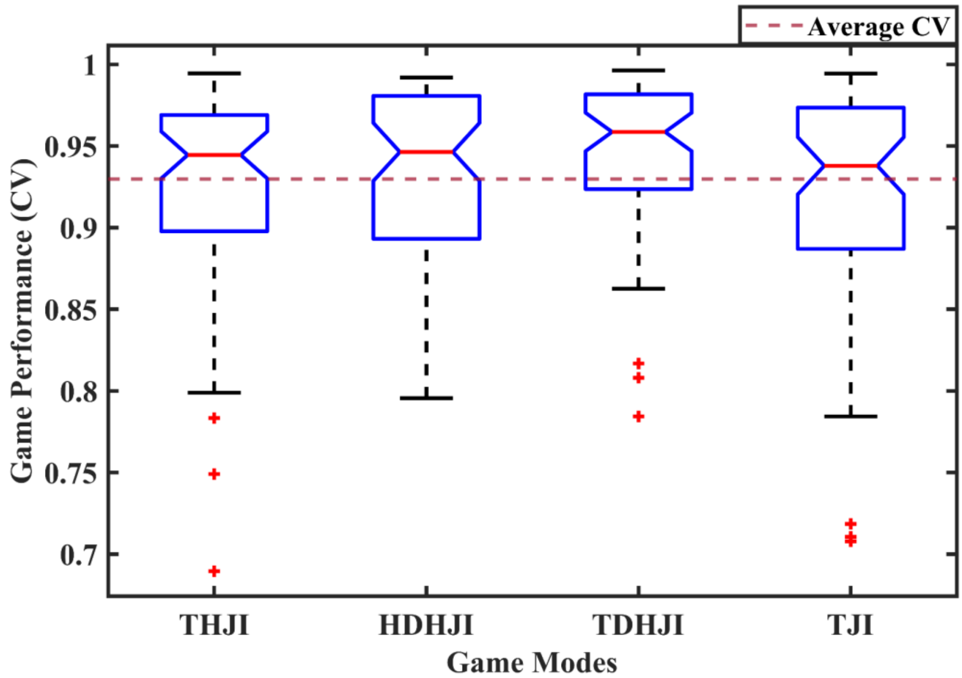

Fig 6.2.3 CV Performance Distribution Over the Game Modes

Fig 6.2.3 shows box plots of CV game performance distribution for every game round included; each box contains 60 data, red lines show the median value, and red crosses define the outliers. On TDHJI rounds, participants showed higher median values showing players had better time synchronizing and performances piled more on the maximum game performance value 1. HDHJI showed similar distribution with the THJI except HDHJI had no outliers helping players to acquire more consistent game performance. TJI showed similar results with THJI, which means improvising as a triad with haptic coupling resulted in the same performance outputs as a duo THJI game mode.

For further investigating the effects of haptic interaction on game performance, average entropy over the game modes has been calculated and correlated with game performance, as the designed nature of the game modes entropy was a key parameter detecting different interaction scenario outputs. It has expected to have maximum entropy on the TJI game rounds, but however TJI showed lower results on entropy levels, and it has seen that players converge into a specific game pattern in every three rounds.

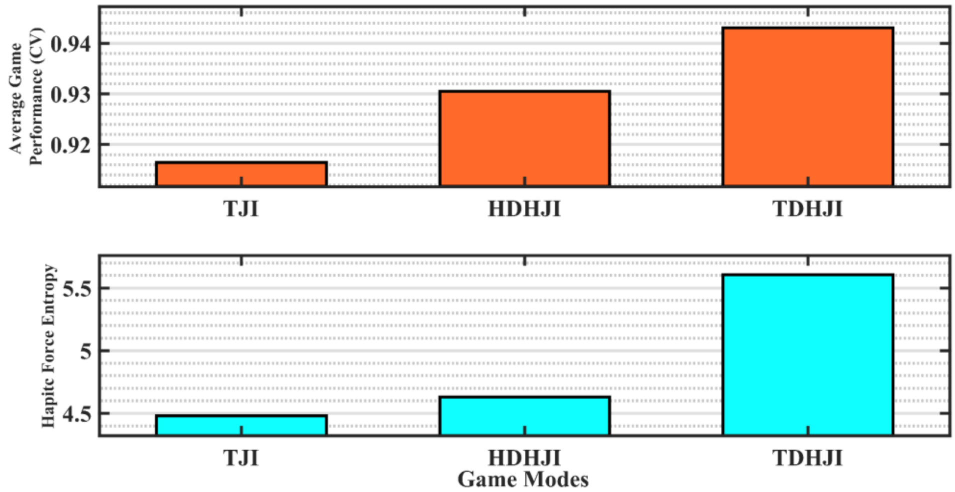

Fig 6.2.4. Haptic Force Entropy Versus Game Performance

Fig 6.2.4 shows average Haptic interaction entropy and average game performance, haptic interaction entropy differences had significant performance improvements in means of synchronization, and prediction capabilities of human players. TJI showed lowest results with haptic interaction entropy resulting lowest game performance on average, HDHJI is in the mid position compared to other game modes resulting higher than TJI and lower than TDHJI. TDHJI has the highest average entropy resulting the top scoring game mode compared the others.

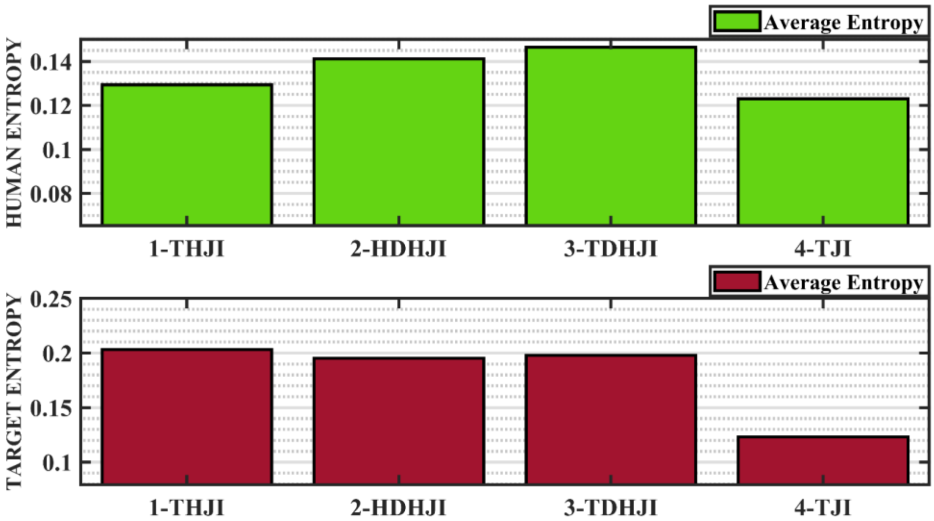

Fig 6.2.5 Human and Target Entropy

Fig 6.2.5 shows the average human and target in-game movement entropy. Haptic interaction entropy also enhanced human movement complexity. In HDHJI human entropy has increased but lowered the average target entropy; with the TDHJI maximum game performance mode, both the players' and the targets' entropy had increased. TJI showed attenuated levels of entropy both in the target and human player.

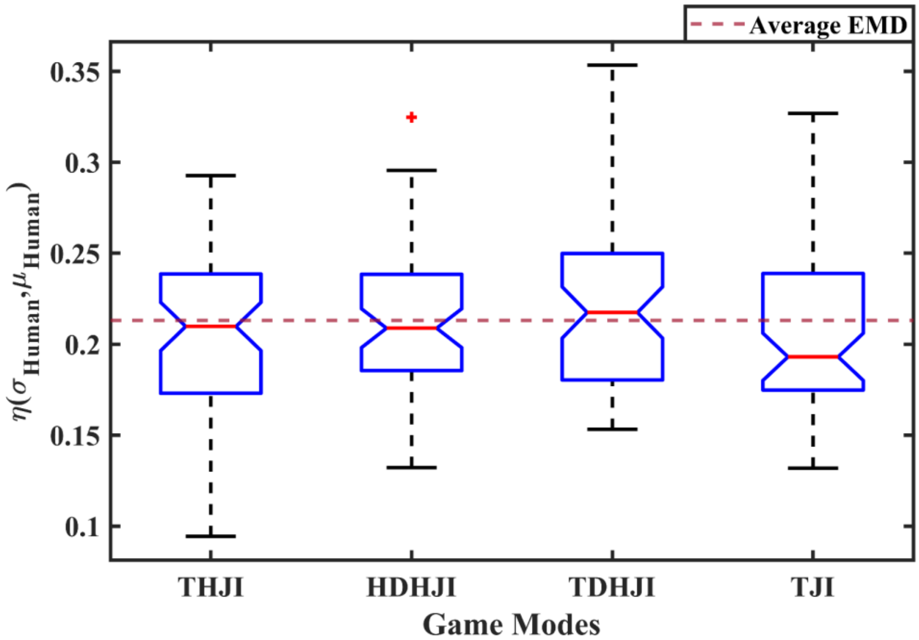

Fig 6.2.6 Human Player In-game and solo round EMD

Fig 6.2.6 shows the distribution of human player in-game and solo round motor signature distances (EMD); each box plot arranged for specific game modes containing 60 pairs of data, black dashed lines indicate the average distance over all game rounds. Higher EMD values mean higher adaptation to in-game signature. On TDHJI rounds, most of the players showed higher adaptation, regarding the median value being higher than the average, also the maximum values of adaptation acquired by this game mode. HDHJI rounds piled on the average, with most of the players playing below the average; the same situation applies for THJI as well. In TJI, players attenuated levels of synchronization, making people harder to adapt to the game.

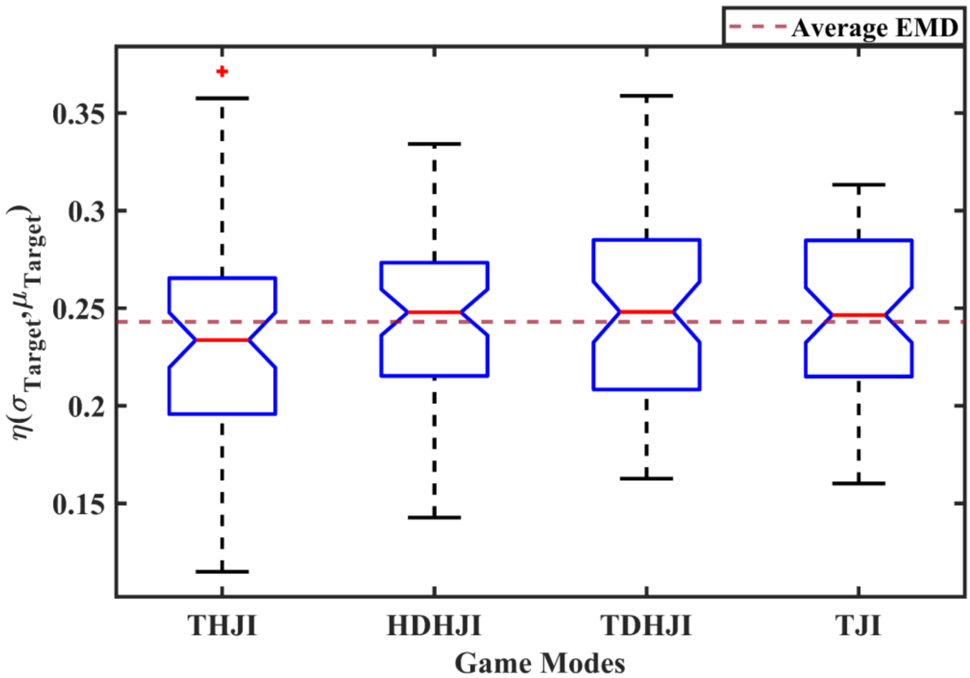

Fig 6.2.7. Target In-game and solo round EMD

Fig 6.2.7 shows the distribution of target in-game and solo round motor signature distances (EMD); each box plot arranged for specific game modes contains 60 pairs of data, and black dashed lines indicate the average distance over all game rounds. Higher EMD values mean higher adaptation to in-game signature. The virtual agent showed better adaptation when the haptic interaction is enabled with the human counterpart; it is a both-way process that benefits both counterparts that unlock good interaction rounds on the mirror game. It is also can be commented that virtual players did not play aggressively, meaning they adapted to human counter parts movements better than human players.

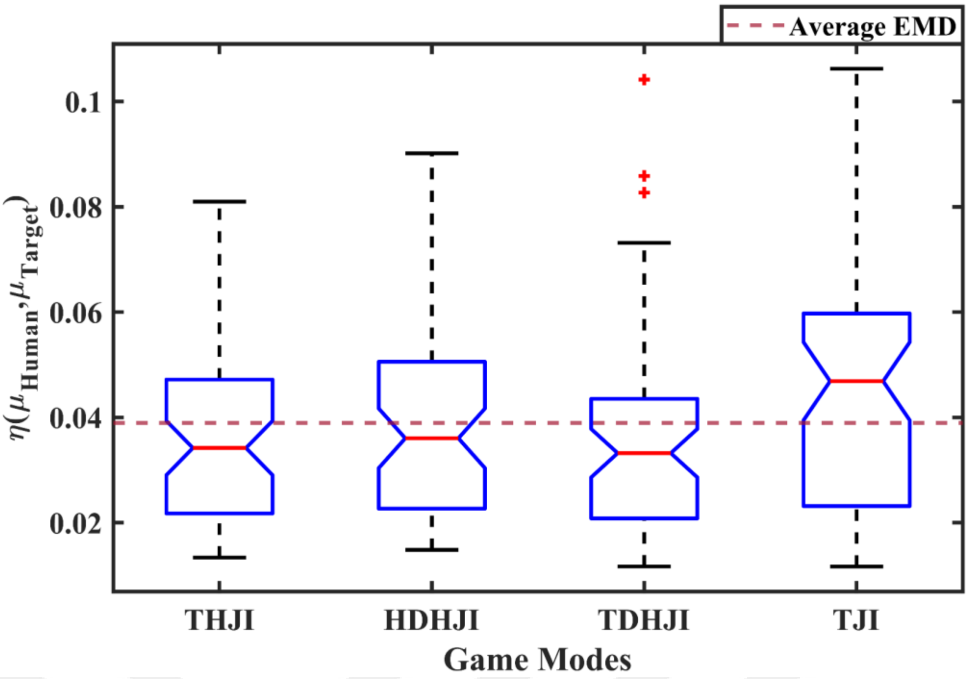

Fig 6.2.8. Target and Human Player round EMD

Fig 6.2.8 shows the distribution of target in-game and solo round motor signature distances (EMD); each box plot is arranged for specific game modes containing 60 pairs of data, and black dashed lines indicate the average distance over all game rounds. Lower EMD values mean higher adaptation to in-game signature. The best performance in means of adaptation showed itself in TDHJI game mode, THJI (H-) showed similar results with HDHJI rounds, TJI has the poorest results in means of in-game adaptation it’s due to different dynamics of the game, target improvising both human player and robot at the same time, it was not possible to focus only on the human player.

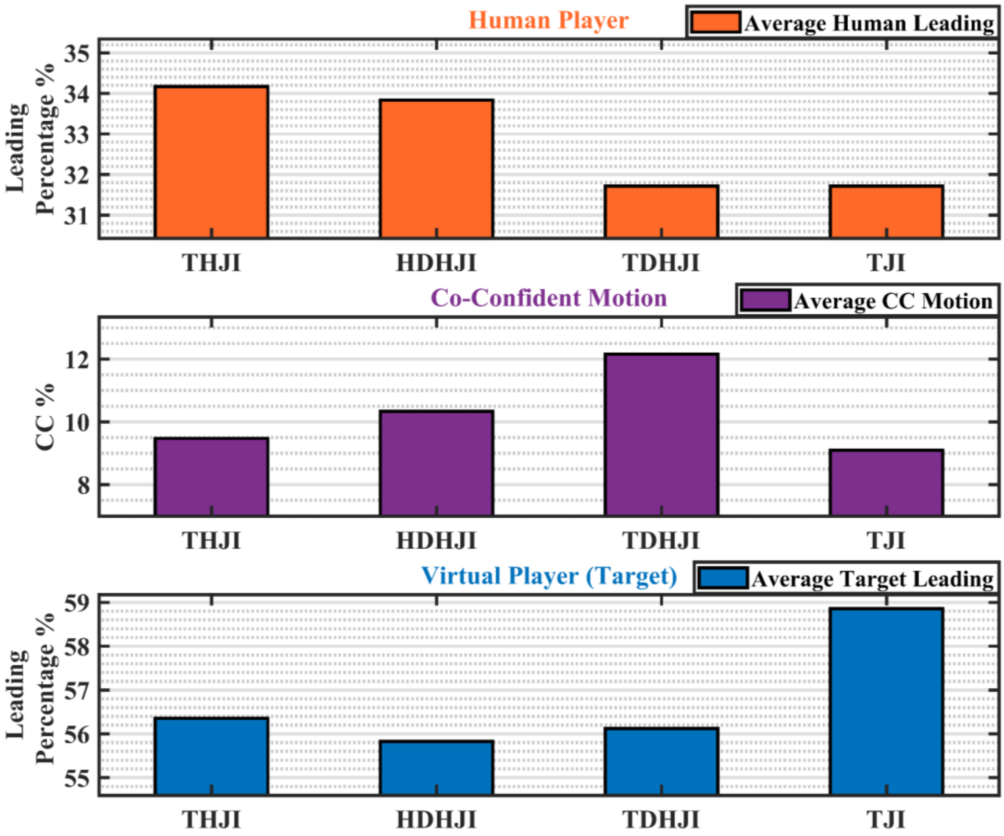

Fig 6.2.9 Game Modes Leading and Co-Confident Motion Percentages

Fig 6.2.9 shows the leading and full synchronization (CC) states of game modes overall on THJI rounds players showed more leading skills compared to other game modes with less co-confident motion states compared to HDHJI and TDHJI. HDHJI players exhibited enhanced synchronization; players didn't give up on their leading patterns; this time target gave up on leading skills and transferred to CC motion. In the highest scoring round TDHJI, players fully unlocked prediction and synchronization capabilities that command made possible by regarding THJI round target leading percentages remained close to THJI rounds, but players' leadership have decreased and increased CC motion states. On TJI rounds, players had attenuated levels of synchronization and leadership due to the target not only improvising with the human player only.

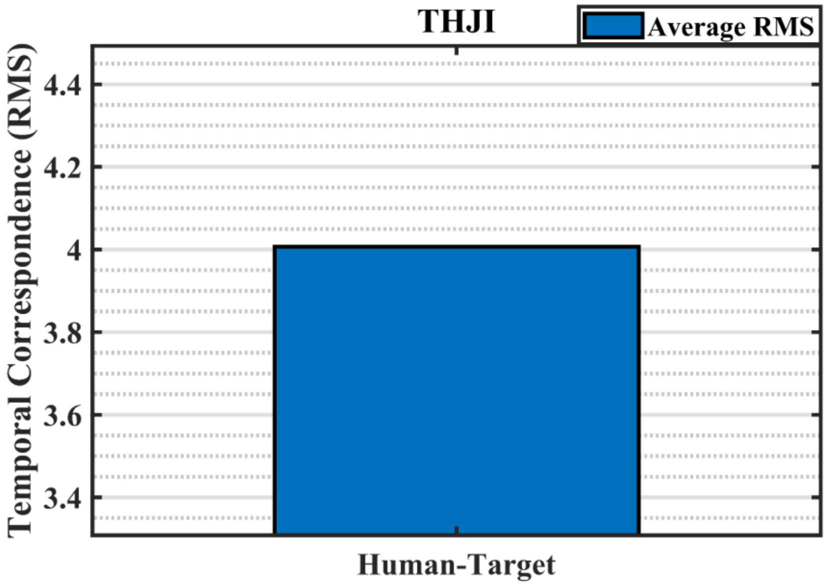

Fig 6.2.10. THJI Human-Target Temporal Correspondence

Fig 6.2.10. shows the average RMS position error between the target and human player; this data will be used for comparison between game modes.

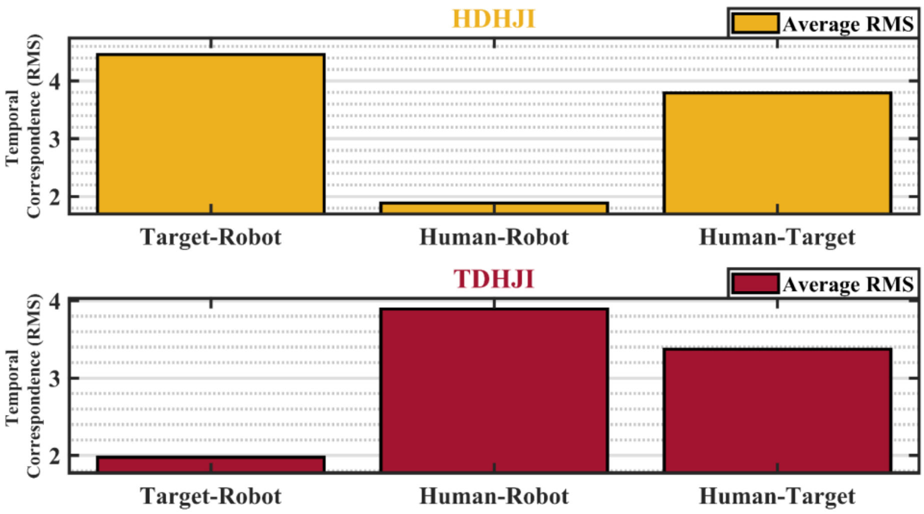

Fig 6.2.11 HDHJI-TDHJI Temporal Correspondence

Fig 6.2.11 shows the average temporal correspondence (RMS) in TDHJI and HDHJI rounds, as expected on HDHJI rounds robot follows human hand movements, which resulted in lower RMS values between human and robot players. HDHJI players had lower average temporal correspondence compared with the Fig 6.2.10 THJI (H-) rounds, which means the players had temporal delay reduction with the help of the haptic interaction scenario in HDHJI. In TDHJI robot follows target movements with the RMS between the target and robot minimized. Human target temporal correspondence is lowest compared to all game modes, resulting TDHJI players having a better time adapting to temporal delays; prediction has increased by the haptic interaction method proposed on TDHJI.

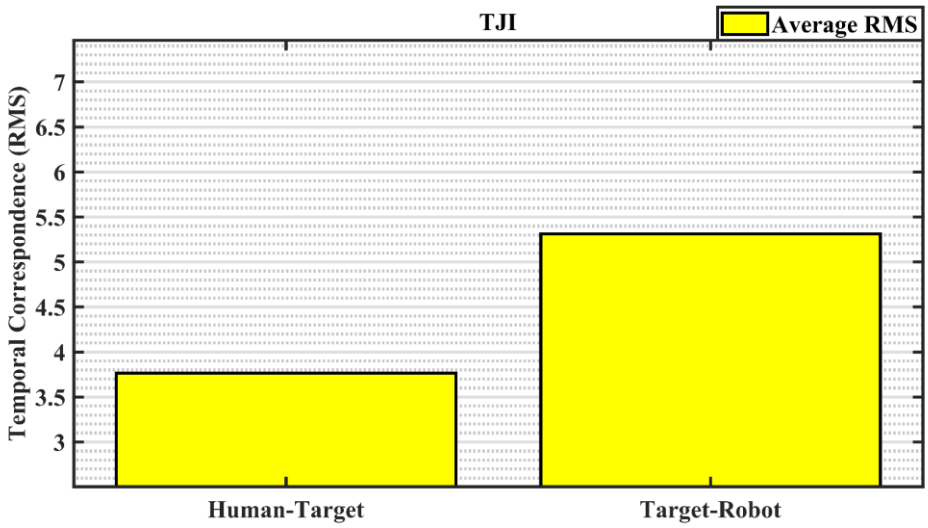

Fig 6.2.12 TJI Temporal Correspondennce

Fig 6.2.12 shows the average temporal correspondence results of the Triad Joint Improvisation game mode. Robot 60% follows the human player, 20% follow the Robot player, and 20% of human co-actors pre-recorded IMS data. That kind of build-up resulted in lower RMS values in Human-Target compared to the Target-Robot player. Human-target RMS showed lower results compared to THJI rounds.

Overall, when haptic interaction enabled any kind of interaction mode evaluated temporal delay adaptation.

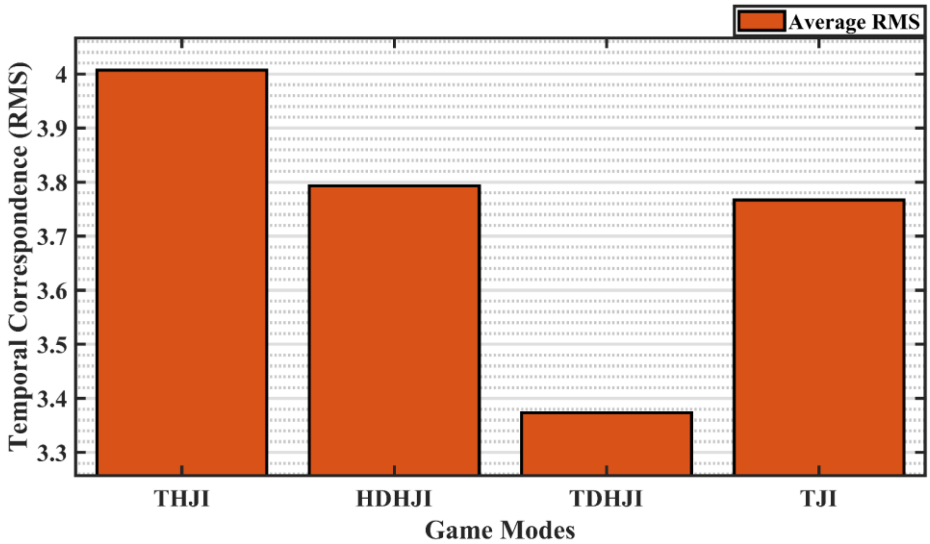

Fig 6.2.13 Average Human-Target RMS Over Game Modes

Co-actors showed 5.33%, 15.8%, and 5.98% improvement in HDHJI, TDHJI, and TJI game modes, respectively; this result also correlates with haptic interaction entropy, haptic interaction enhanced human player temporal delay adaptation and prediction capabilities.

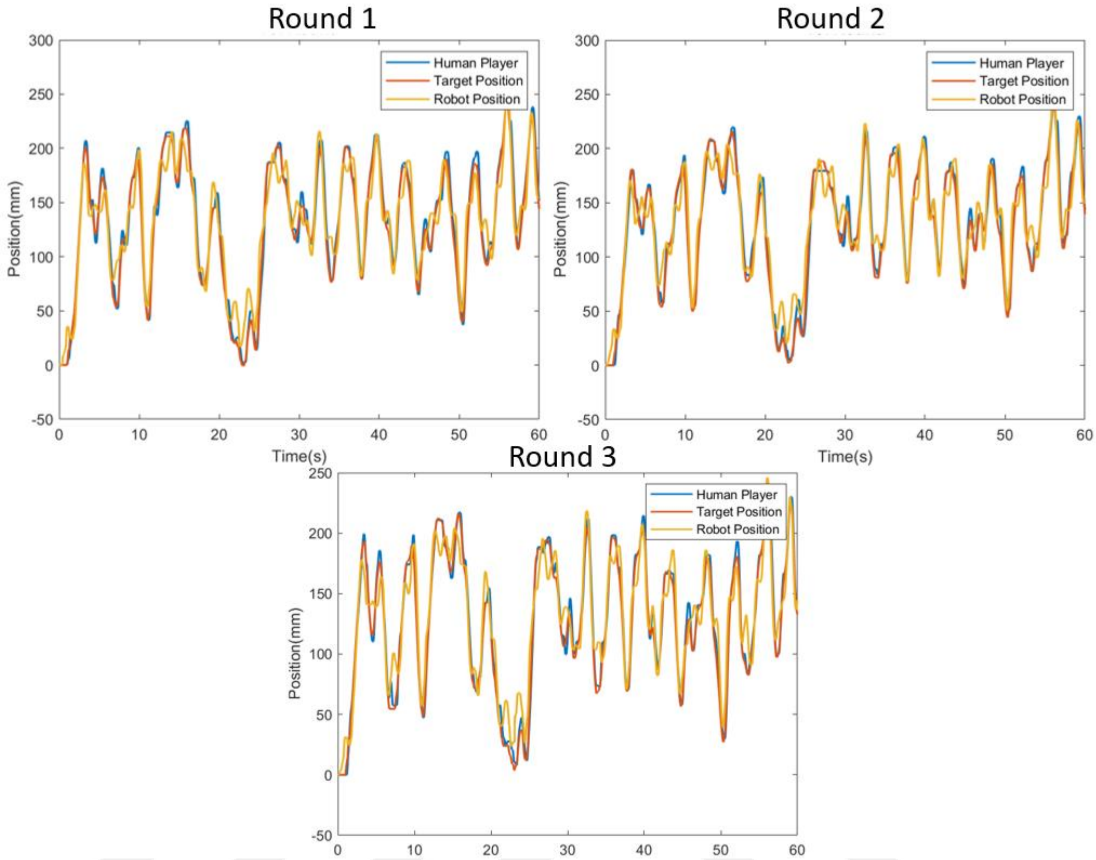

Fig 6.2.14 TJI Pattern Generation

Fig 6.2.14 shows Dyad 6's pattern generation over the game rounds; players have converged to a specific pattern with the triad joint improvisation game mode, and those patterns are generated due to the human player motor signature and robot motor signature; these results may contain specific joint action cues since it is specific for every player in game rounds. However, improvising as a triad needs to be tested among human players only for detecting the same kind of pattern generation.

CHAPTER 7

STATISTICAL ANALYSIS

All statistical analyses were performed using JAMOVI [62-64].

For statistical analyses, performance in the JI-MG were investigated by repeated measures analysis of variance (RM-ANOVA), where 3 rounds of the JI-MG were set as the repeated factor with 3 levels, 4 different modes of the JI-MG (THJI, HDHJI, TDHJI and TJI) were set as the between-subjects factor and Circular Variance (CV), Co-Confident Motion (CC), Haptic Entropy (HE), Human EMD(HEMD), Virtual Player-Target EMD (VPEMD), and Temporal Correspondence (RMS) were the dependent variables. The sphericity assumption was checked for each RM-ANOVA run by Mauchly's W value and its level of significance. When p value of Mauchly's W was < .05, Greenhouse-Geisser correction was used for the F values.

7.1 Circular Variance

The RM-ANOVA for CV showed that neither the rounds, nor the mirror game modes had a significant effect on the CV values (F_{Rounds} (2, 152) = 1.083, p = 0.341, η^2p = 0.014; $F_{MG\ modes}$ (3, 76) = 0.662, p = 0.578, η^2p = 0.025, respectively)

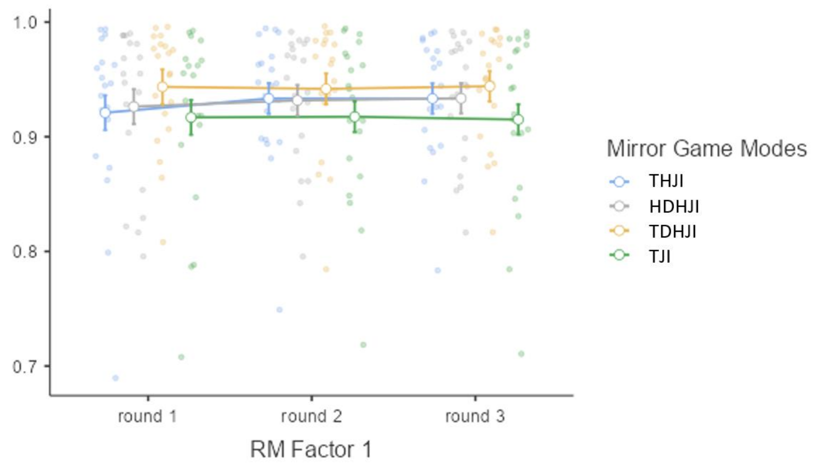

Fig 7.7.1 Estimated marginal mean values of CV.

Fig 7.1.1 Estimated marginal mean values of CV are shown. Different colors represent the MG modes and different color data points correspond to CV values obtained in corresponding mirror game mode. Bars represent the 95 % confidence interval.

7.2 In-Game EMD

The RM-ANOVA for in-game EMD showed that neither the rounds, nor the mirror game modes had a significant effect on the in-game EMD values (F_{Rounds} (2, 152) = 1.751, p = 0.177, $\eta^2 p$ = 0.023; $F_{MG\ modes}$ (3, 76) = 0.652, p = 0.584, $\eta^2 p$ = 0.025, respectively).

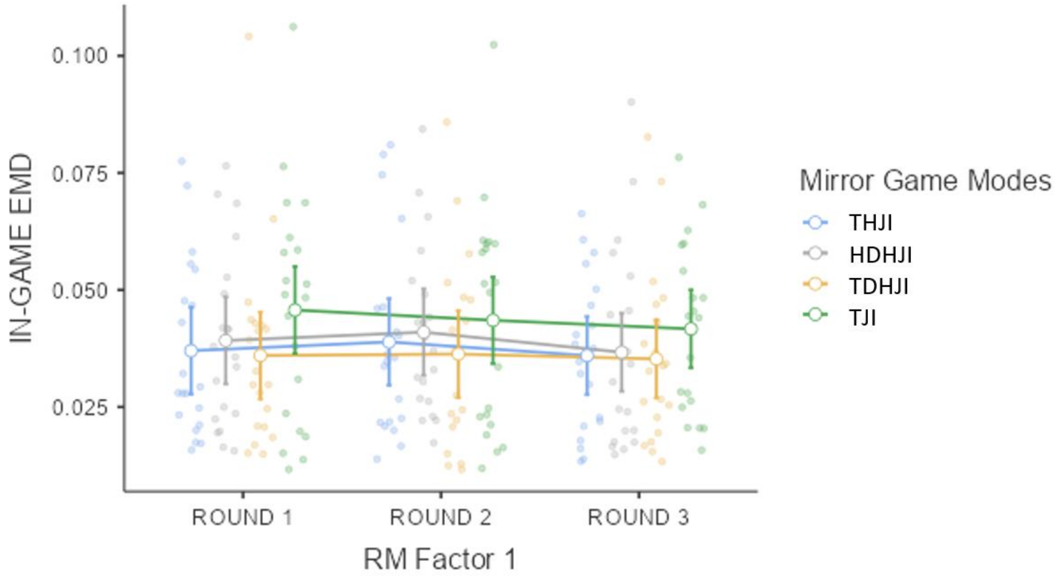

Fig 7.2.1 Estimated marginal mean values of in-game EMD.

Fig 7.2.1 Estimated marginal mean values of in-game EMD are shown. Different colors represent the MG modes and different color data points correspond to in-game EMD values obtained in corresponding mirror game mode. Bars represent the 95 % confidence interval.

7.3 Haptic Entropy

The RM-ANOVA for Haptic Entropy showed the rounds did not have a significant effect (F_{Rounds} (2, 114) = 0.9223, p = .401, $\eta^2 p$ = 0.016. But the mirror game modes had a significant effect on the HE values ($F_{MG\ modes}$ (2, 57) = 22.2, p < .001, $\eta^2 p$ = 0.438). The interaction between rounds and MG modes was also not significant ($F_{Rounds*MG\ Modes}$ (4, 114) = 0.0805, p = .988, $\eta^2 p$ = 0.003).

For the post-hoc comparison of mirror game modes, LSD comparisons indicated that TDHJI (*M* = 5.606, *SD* = 0.130) had significantly higher HE values compared to HDHJI (*M* = 4.629, *SD* = 0.130) and TJI (*M* = 4.959, *SD* = 0.130). The HE values of HDHJI and TJI did not differ significantly.

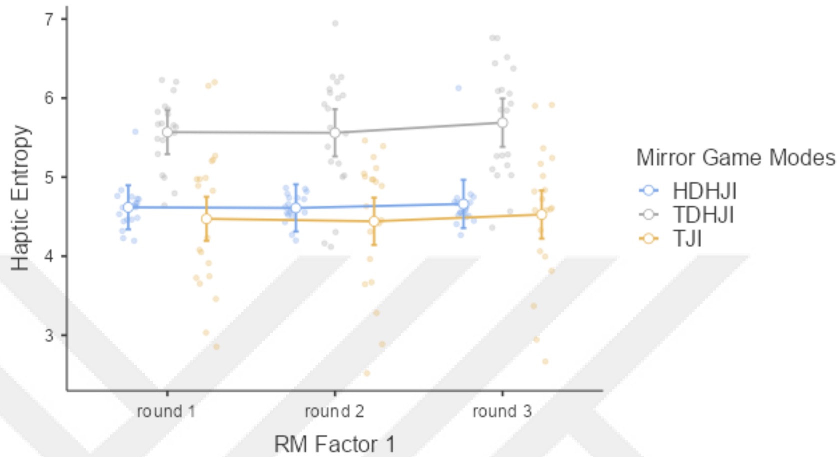

Fig 7.3.1 Estimated marginal mean values of HE

Fig 7.3.1 Estimated marginal mean values of HE is shown. Different colors represent the MG modes and different color data points correspond to HE values obtained in corresponding mirror game mode. Bars represent the 95 % confidence interval.

7.4 Human EMD

The RM-ANOVA for Human EMD showed that neither the rounds, nor the mirror game modes had a significant effect on the HEMD values (F_{Rounds} (2, 152) = 1.759, p = 0.176, $\eta^2 p$ = 0.023; $F_{MG\ modes}$ (3, 76) = 0.521, p = 0.669, $\eta^2 p$ = 0.025, respectively).

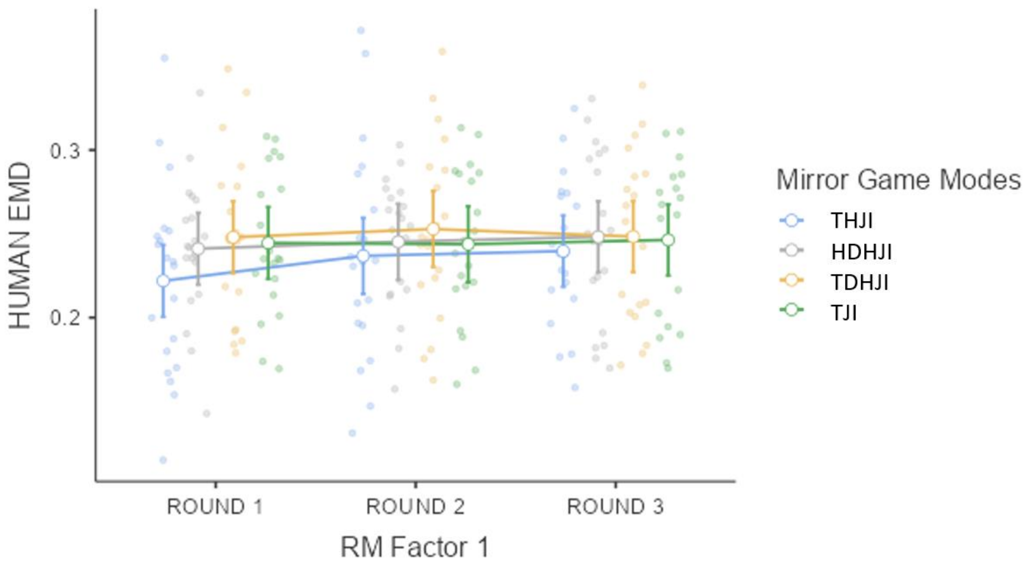

Fig 7.4.1 Estimated marginal mean values of HEMD

Fig 7.4.1 Estimated marginal mean values of HEMD are shown. Different colors represent the MG modes and different color data points correspond to HEMD values obtained in corresponding mirror game mode. Bars represent the 95 % confidence interval.

7.5 VP EMD

The RM-ANOVA for VP EMD showed the rounds had a significant effect (F_{Rounds} (2, 152) = 3.626, p = 0.029, η^2p = 0.046) but the mirror game modes did not have a significant effect on the VPEMD values ($F_{MG\ modes}$ (3,76) = 0.578, p = 0.631, η^2p = 0.022). The interaction between rounds and the game modes was also not significant for the VPEMD values ($F_{Rounds\ *MG\ modes}$ (6, 152) = 0.886, p = 0.507, η^2p = 0.034, respectively)

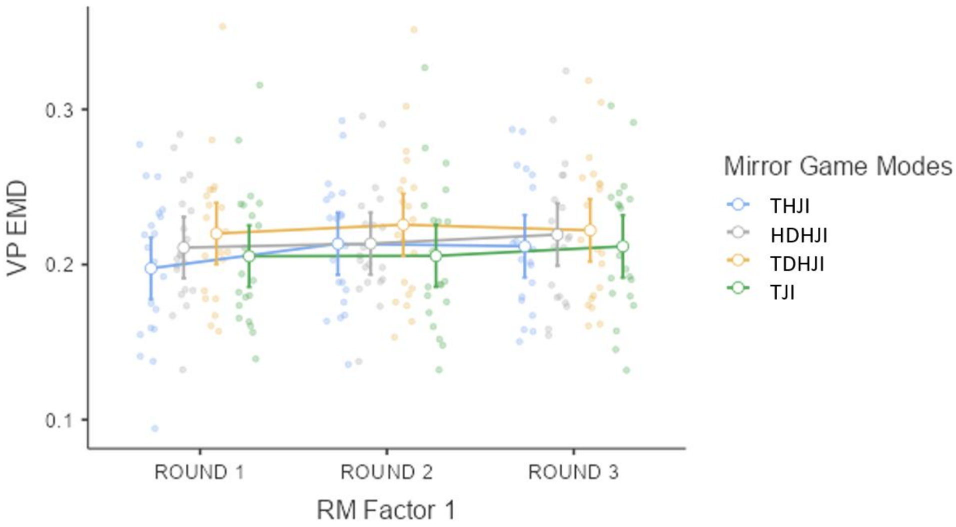

Fig 7.5.1 Estimated marginal mean values of VP EMD

Fig 7.5.1 Estimated marginal mean values of VP EMD are shown. Different colors represent the MG modes and different color data points correspond to VP EMD values obtained in corresponding mirror game mode. Bars represent the 95 % confidence interval.

The post-hoc comparison indicated that round 3 (*M* = 0.216, *SD* = 0.005) had significantly higher mean VP EMD value than round 1 (*M* = 0.208, *SD* = 0.005) but not from round 2 (*M* = 0.215, *SD* = 0.005). HEMD values did not significantly differ between round 2 and round 3.

7.6 RMS

The RM-ANOVA for RMS showed that neither the rounds, nor the mirror game modes had a significant effect on the RMS values (F_{Rounds} (2, 152) = 2.264, p = 0.055, η^2p = 0.023; $F_{MG\ modes}$ (3, 76) = 1.986, p = 0.069, η^2p = 0.027, respectively).

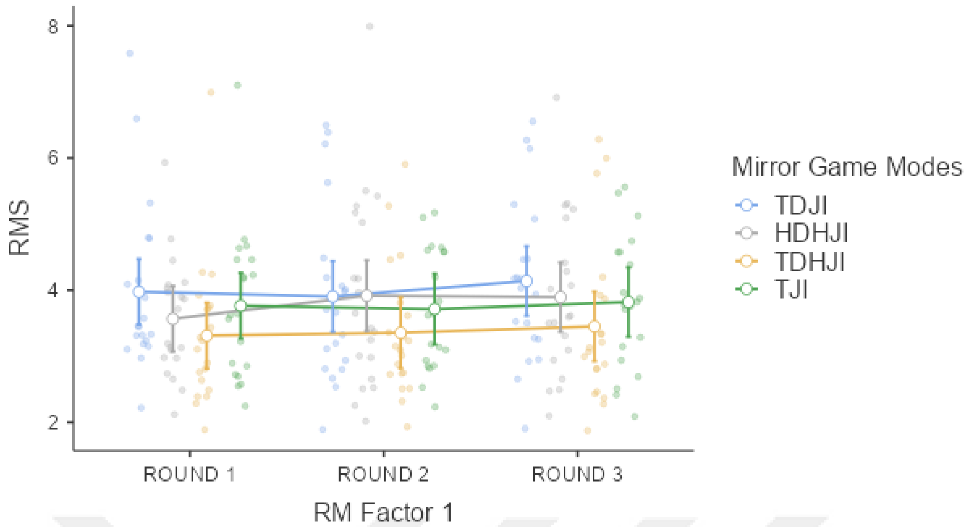

Fig 7.2.1 Estimated marginal mean values of RMS

Fig 7.6.1 Estimated marginal mean values of RMS are shown. Different colors represent the MG modes and different color data points correspond to RMS values obtained in corresponding mirror game mode. Bars represent the 95 % confidence interval.

7.7 CC

The RM-ANOVA for CC showed that neither the rounds, nor the mirror game modes had a significant effect on the CC values (F_{Rounds} (2, 152) = 1.542, p = 0.075, $\eta^2 p$ = 0.045; $F_{MG\ modes}$ (3, 76) = 1.672, p = 0.082, $\eta^2 p$ = 0.054, respectively).

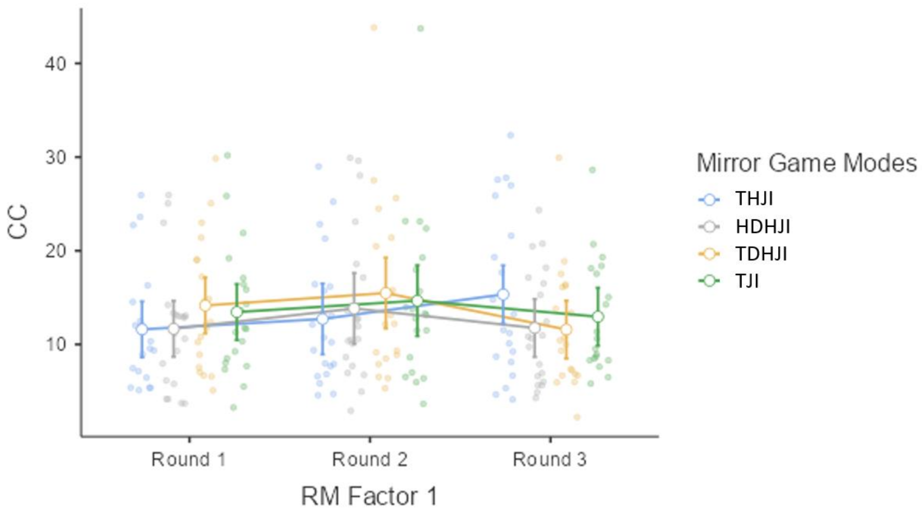

Fig 7.2.1 Estimated marginal mean values of CC

Fig 7.7.1 Estimated marginal mean values of CC are shown. Different colors represent the MG modes and different color data points correspond to CC values obtained in corresponding mirror game mode. Bars represent the 95 % confidence interval.

CHAPTER 8

CONCLUSIONS

8.1 Remarks

This study is motivated to understand, imitate, and enhance human coordination mechanics in joint improvisation modality with the aid of virtual players. Virtual players employ a mathematical Central Pattern Generator imitating a biological neural mammalian pattern generation system. Programmable CPG network enhanced with the exit from synchrony term to imitate nature of coordinated movements, also individual motor signature has added to mimic specific human movement characteristics.

Virtual environment experimental set-up developed using a virtual medium on Simulink, using similar mirror game approaches, for design; two parallel tracks and ball avatars with 1 DOF controlled with a joystick. A new haptic interaction scenario is introduced, coupling two improvising players together. Improvising CPG architecture implemented for virtual players with a play style as using a joystick. Haptic interaction enhanced human player performances by means of synchronization.

Experimental set-up developed using physical game components that players can interact with. 1 DOF robot arm implemented for haptic interaction and different play scenarios. Improvising CPG architecture is implemented in the robot arm and target with adjustable weights that can affect interaction during the game. Five scenarios are created on PE experimental rig for studying improvisation, namely Solo, Target-Human, Human Driven Haptic, Target Driven Haptic, and Triad Joint improvisation. Haptic interaction entropy is enabled as a key mechanism in studying scenarios, using THJI as a control group where there is no haptic interaction between robot and human, regardless of the game round; when haptic interaction is enabled, players showed better temporal delay compensation (RMS). TDHJI had the most complex haptic feedback to human players and showed the best results in temporal delay compensation (RMS), game performance (CV), and motor signature adaptation, with similar results for the virtual agent (target). HDHJI game mode comes at the second stage with lower haptic entropy and showed better results in motor signature adaptation and game performance (CV) compared to THJI rounds. TJI is generated as a new play style in mirror game even though game performance is lower than players had better temporal delay adaptation.

8.2 Future works

This work can be improved through the future thesis with the following ideas.

- Playing weights of CPGs can be optimized for best human-like play styles.
- Different game modes can be introduced to study Triad Joint Improvisation
- Data must be evaluated for non-typically developed humans, such as ASD or anxiety.
- Dyads must be increased for better results of ANOVA Analysis.
- Different methods should be generated for individual motor signature embedding to virtual agents.
- It can be studied if the movement enhancements are permanent in the mirror game.
- Moments of co-confident motion can be monitored using functional near-infrared spectroscopy to investigate temporal delay adaptation and prediction mechanisms.
- Psychological markers can be investigated for better detection of co-confident motion states.
- A new method can be delivered to study triad improvisation among only human players in mirror game.
- Effects of haptic interaction entropy can be studied between typically developed and non-typically developed human beings.
- The cerebellum's role in MG can be evaluated using transcranial direct current stimulation (tDCS) on the subjects.
- A process can be added to assess psychological status of players such as in [26]

REFERENCES

[1] R. C. Schmidt, and M. J. Richardson, "Dynamics of interpersonal coordination," *In Coordination: Neural, behavioral and social dynamics*, pp. 281-308, 2008.

[2] Feniger-Schaal, R., Noy, L., Hart, Y., Koren-Karie, N., Mayo, A. E., & Alon, U. (2016). Would you like to play together? Adults' attachment and the mirror game. Attachment & human development, 18(1), 33-45.

[3] Varlet, M., Marin, L., Capdevielle, D., Del-Monte, J., Schmidt, R., Salesse, R., ... & Raffard, S. (2014). Difficulty leading interpersonal coordination: towards an embodied signature of social anxiety disorder. Frontiers in Behavioral Neuroscience, 8, 29.

[4] Lavelle, M., Healey, P. G., & McCabe, R. (2013). Is nonverbal communication disrupted in interactions involving patients with schizophrenia? Schizophrenia bulletin, 39(5), 1150-1158

[5] Del-Monte, J., Capdevielle, D., Varlet, M., Marin, L., Schmidt, R. C., Salesse, R. N., ... & Raffard, S. (2013). Social motor coordination in unaffected relatives of schizophrenia patients: a potential intermediate phenotype. Frontiers in behavioral neuroscience, 7, 137.

[6] Problovski, H. Z. G., Lavi, D., Yozevitch, R., Sherman, M., Hagay, Y., & Dahan, A. (2021). Impairments of interpersonal synchrony evident in attention deficit hyperactivity disorder (ADHD). Acta Psychologica, 212, 103210.

[7] O'Doherty, J., Winston, J., Critchley, H., Perrett, D., Burt, D. M., and Dolan, R. J. (2003). Beauty in a smile: the role of medial orbitofrontal cortex in facial attractiveness. Neuropsychologia 41, 147–55.

[8] R. P. R. D. van der Wel, G. Knoblich, and N. Sebanz, “Let the force be with us: Dyads exploit haptic coupling for coordination,” *Journal of Experimental Psychology: Human Perception and Performance*, vol. 37, no. 5, pp. 1420–1431, 2011.

[9] G. Ganesh, A. Takagi, R. Osu, T. Yoshioka, M. Kawato, and E. Burdet, “Two is better than one: Physical interactions improve motor performance in humans,” *Scientific Reports*, vol. 4, Jan. 2014.

[10] A. Takagi, G. Ganesh, T. Yoshioka, M. Kawato, and E. Burdet, “Physically interacting individuals estimate the partner’s goal to enhance their movements,” *Nature Human Behaviour*, vol. 1, no. 3, Mar. 2017.

[11] Noy (2011) The mirror game as a paradigm for studying the dynamics of two people improvising motion together, Proceedings of the National Academy of Sciences of the United States of America; 108(52)

[12] Haken H., Kelso J. A. S. A. S., & Bunz H. (1985). A theoretical model of phase transitions in human hand movements. Biological Cybernetics, 51(5), 347–356. doi: 10.1007/BF00336922 PMID: 3978150

[13] Righetti, L., & Ijspeert, A. J. (2006). Programmable central pattern generators: An application to biped locomotion control. Proceedings 2006 IEEE International Conference on Robotics and Automation, 2006. ICRA 2006.

[14] Dahan, A., Noy, L., Hart, Y., Mayo, A., & Alon, U. (n.d.). Exit from synchrony in joint improvised motion. PLOS ONE

[15] Slowinski, P., Rooke, E., Di Bernardo, M., & Tanaseva-Atanasova, K. (2014, October). Kinematic characteristics of motion in the mirror game. In 2014 IEEE International Conference on Systems, Man, and Cybernetics (SMC) (pp. 748-753). IEEE. doi: 10.1109/SMC.2014.6974000.

[16] Słowiński, P., Zhai, C., Alderisio, F., Salesse, R., Gueugnon, M., Marin, L., ... & Tsaneva-Atanasova, K. (2016). Dynamic similarity promotes interpersonal coordination in joint action. Journal of The Royal Society Interface, 13(116), 20151093. doi: 10.1098/rsif.2015.1093

[17] C. Zhai, F. Alderisio, P. Słowiński, K. Tsaneva-Atanasova, and M. di Bernardo, M. “Design of a virtual player for joint improvisation with humans in the mirror game,” PloS one, 11(4), e0154361, 2016.

[18] Morris, J. S., Frith, C. D., Perrett, D. I., Rowland, D., Young, A. W., Calder, A. J., et al. (1996). A differential response in the human amygdala to fearful and happy facial expressions. Nature 383, 812–15

[19] Phillips, M. L., Young, A. W., Senior, C., Brammer, M., Andrew, C., Calder, A. J., et al. (1997). A specified neural substrate for perceiving facial expressions of disgust. Nature 389, 495–8.

[20] Sprengelmeyer, R., Rausch, M., Eysel, U. T. and Przuntek, H. (1998). Neural structures associated with the recognition of facial basic emotions. Proc. R. Soc. Lond. B 265, 1927–31. (DOI 10.1098/rspb.1998.0522.)

[21] Winston, J. S., Strange, B. A., O’Doherty, J., and Dolan, R. J. (2002). Automatic and intentional brain responses during evaluation of trustworthiness of faces. Nat. Neurosci. 5, 277–83.

[22] Phelps, E. A. (2001). Faces and races in the brain. Nat. Neurosci. 4, 775–6

[23] O'Doherty, J., Winston, J., Critchley, H., Perrett, D., Burt, D. M., and Dolan, R. J. (2003). Beauty in a smile: the role of medial orbitofrontal cortex in facial attractiveness. Neuropsychologia 41, 147–55.

[24] F. J. Bernieri, "Coordinated movement and rapport in teacher-student interactions," Journal of Nonverbal behavior, 12(2), 120-138, 1988.

[25] Gallese, V., Fadiga, L., Fogassi, L., and Rizzolatti, G. (1996). Action recognition in the premotor cortex. Brain 119, 593–609.

[26] Rizzolatti, G., Fadiga, L., Gallese, V., and Fogassi, L. (1996). Premotor cortex and the recognition of motor actions. Brain Res. Cogn. 3, 131–41.

[27] D'Ausilio A., Novembre G., Fadiga L., Keller P. E. (2015). What can music tell us about social interaction? Trends in Cognitive Sciences, 19, 111–114.

[28] Wheatley, T., Kang, O., Parkinson, C., & Looser, C. E. (2012). From mind perception to mental connection: Synchrony as a mechanism for social understanding. Social and Personality Psychology Compass, 6(8), 589-606. doi: 10.1111/j.1751-9004.2012.00450.x

[29] Kourtis D., Knoblich G., Wozniak M., Sebanz N. (2014). Attention allocation and task representation during joint action planning. Journal of Cognitive Neuroscience, 26(10), 2275–2286.

[30] Sacheli L. M., Arcangeli E., Paulesu E. (2018). Evidence for a dyadic motor plan in joint action. Scientific Reports, 8, Article 5027. https://doi.org/10.1038/s41598-018-23275-9

[31] Kourtis D., Woźniak M., Sebanz N., Knoblich G. (2019). Evidence for we-representations during joint action planning. Neuropsychologia, 131, 73–83

[32] Tsai C., Sebanz N., Knoblich G. (2011). The GROOP effect: Groups mimic group actions. Cognition, 118, 135–140.

[33] Loehr J. D., Kourtis D., Vesper C., Sebanz N., Knoblich G. (2013). Monitoring individual and joint action outcomes in duet music performance. Journal of Cognitive Neuroscience, 25, 1049–1061.

[34] Wolf T., Sebanz N., Knoblich G. (2018). Joint action coordination in expert-novice pairs: Can experts predict novices' suboptimal timing? Cognition, 178, 103–108.

[35] J. Issartel, M. Gueugnon, and L. Marin, "Understanding the impact of expertise in joint and solo-improvisation," Frontiers in Psychology, 8, 1078. 2017.

[36] R. Duarte, D. Araújo, K. Davids, B. Travassos, V. Gazimba, and J. Sampaio, "Interpersonal coordination tendencies shape 1-vs-1 sub-phase performance outcomes in youth soccer," Journal of sports sciences, 30(9), 871-877, 2012.

[37] I. Brinck "Joint improvisation in the arts practices: Entrainment, engagement, and expert skill." Proceedings of A Body of Knowledge, 2018.

[38] Gueugnon M, Salesse RN, Coste A, Zhao Z, Bardy BG, Marin L (2016) The acquisition of socio-motor improvisation in the mirror game. Hum Mov Sci. 46:117-28.

[39] M. J. Matari, and B. Scassellati, “Socially Assis 1973 Part G ” 73. Socially Assistive Robotics, 2019.

[40] K. Dautenhahn, C.L. Nehaniv, M. L. Walters, B. Robins, H. Kose-Bagci, N. Assif, and M. Blow, “KASPAR–a minimally expressive humanoid robot for human–robot interaction research,” Applied Bionics and Biomechanics, 6(3, 4), 369-397, 2009

[41] “Post-Stroke Rehabilitation Fact Sheet | National Institute of Neurological Disorders and Stroke.” Nih.Gov., 2012

[42] Euromov.eu, ”What is AlterEgo project ?”, 2013. [Online]. Available: http://www.euromov.eu/alterego/project. [Accessed: 30- Jul- 2015].

[43] Noy, L., Levit-Binun, N., & Golland, Y. (2015). Being in the zone: physiological markers of togetherness in joint improvisation. Frontiers in human neuroscience, 9, 187.

[44] Noy, L., Weiser, N., & Friedman, J. (2017). Synchrony in joint action is directed by each participant’s motor control system. Frontiers in psychology, 8, 531. doi:10.3389/fpsyg.2017.00531

[45] M. Khoramshahi, A. Shukla and A. Billard, “Cognitive mechanism in synchronized motion: An internal predictive model for manual tracking control (special session),” 2014 IEEE International Conference on Systems, Man, and Cybernetics (SMC), San Diego, CA, 2014, pp. 765-771, doi: 10.1109/SMC.2014.6974003

[46] Tagaki, A., Ganesh, G., Yoshioka, T., Kawato, M., Burdet E. (2017) “Physically interacting individuals estimate the partner’s goal to enhance their movements,” Nat. Hum. Behav., 1, 0054, pp.1-6.

[47] Sebanz, N., Bekkering, H., Knoblich, G. (2006) “Joint Action: Bodies and minds moving together”, Trends Cong. Sci., 10, pp.70-76

[48] Brezis, R. S., Noy, L., Alony, T., Gotlieb, R., Cohen, R., Golland, Y., & Levit-Binnun, N. (2017). Patterns of joint improvisation in adults with autism spectrum disorder. Frontiers in psychology, 8, 1790. doi:10.3389/fpsyg.2017.01790

[49] Lanini, J., Duburcq, A., Razavi, H., Goff, C. G. L., and Ijspeert, A. J. (2017). Interactive locomotion: Investigation and modeling of physically-paired humans while walking. PLoS ONE 12:e179989. doi: 10.1371/journal.pone.0179989

[50] Sylos-Labini, F., d’Avella, A., Lacquaniti, F., and Ivanenko, Y. (2018). Human- human interaction forces and interlimb coordination during side-by-side walking with hand contact. Front. Physiol. 9:179. doi: 10.3389/fphys.2018. 00179

[51] Schmidt R. C., & Richardson M. J. (2008). Dynamics of interpersonal coordination. In Coordination: Neural, behavioral and social dynamics (pp. 281–308). Springer Berlin Heidelberg doi: 10.1007/978- 3-540-74479-5_14

[52] Oullier O., de Guzman G. C., Jantzen K. J., Lagarde J., & Kelso J. A. S. (2008). Social coordination dynamics: Measuring human bonding. Social Neuroscience, 3(2), 178–192. doi: 10.1080/ 17470910701563392 PMID: 18552971

[53] Schmidt R. C., Carello C., & Turvey M. T. (1990). Phase Transitions and Critical Fluctuations in the Visual Coordination of Rhythmic Movements Between People, 16(2), 227–247 PMID: 2142196

[54] Kelso JAS (1995) Dynamic patterns: The self-organization of brain and behavior. MIT Press, Cambridge.

[55] Alderisio, F., Antonacci, D., Zhai, C., & di Bernardo, M. (2016, June). Comparing different control approaches to implement a human-like virtual player in the mirror game. In 2016 European Control Conference (ECC) (pp. 216-221). IEEE. doi: 10.1109/ECC.2016.7810289.

[56] Hart Y., Noy L., Feniger-Schaal R., Mayo A. E., & Alon U. (2014). Individuality and togetherness in joint improvised motion. PloS one, 9(2), e87213. doi: 10.1371/journal.pone.0087213 PMID: 24533054

[57] Wojcik, Jeremy; Clewley, Robert; Shilnikov, Andrey (16 May 2011). “Order parameter for bursting polyrhythms in multifunctional central pattern generators”. Physical Review E. 83 (5): 056209. Bibcode:2011PhRvE..83e6209W.

[58] Hooper, Scott L. (1999–2010). “Central Pattern Generators”. Encyclopedia of Life Sciences. John Wiley & Sons. doi:10.1038/npg.els.0000032. ISBN 978-0-470-01590-2.

[59] Prochazka A, Ellaway PH (2012). “Sensory systems in the control of movement”. Comprehensive Physiology, Supplement 29: Handbook of Physiology, Exercise: Regulation and Integration of Multiple Systems.

[60] Lamb, P. F., & Stöckl, M. (2014). On the use of continuous relative phase: Review of current approaches and outline for a new standard. Clinical Biomechanics, 29(5), 484-493.

[61] ME435 Mechatronics Lecture Notes

[62] The jamovi project (2022). jamovi. (Version 2.3) [Computer Software]. Retrieved from https://www.jamovi.org.

[63] R Core Team (2021). R: A Language and environment for statistical computing. (Version 4.1) [Computer software]. Retrieved from https://cran.r-project.org. (R packages retrieved from MRAN snapshot 2022-01-01).

[64] Singmann, H. (2018). afex: Analysis of Factorial Experiments. [R package]. Retrieved from https://cran.r-project.org/package=afex.